Spring Precipitation Deficits Exacerbate Streamflow Declines in the Upper Colorado River Basin During the Millennium Drought

Daniel Hogan

A thesis

submitted in partial fulfillment of the

requirements for the degree of

Master of Science

University of Washington

2023

Committee:

Jessica Lundquist

Bart Nijssen

Program Authorized to Offer Degree:

Civil and Environmental Engineering

University of Washington

Abstract

Spring Precipitation Deficits Exacerbate Streamflow Declines in the Upper Colorado River Basin During the Millennium Drought

Daniel Hogan

Chair of Supervisory Committee:
Jessica Lundquist
Civil and Environmental Engineering

The Colorado River heavily relies on the annual pulse of snowmelt from the Rocky Mountains within the Upper Colorado River Basin (UCRB), where over 90% of streamflow originates. Since 2000, the Colorado River has been delivering less water per unit precipitation than in preceding decades. The over 40 million people reliant on this water are concerned, where did that water go? Prior research has suggested the water loss is linked to warming temperatures, but prior work has not focused on the importance of seasonality in snow-dominated basins, which provide over 80% of Colorado River water. Spring weather must be considered because it controls when snow melts and how much energy is available for evaporation when the soil is wettest. These impacts make spring weather a critical contributor to annual streamflow. We found the most significant drop in seasonal precipitation since 2000 was during spring, with a decrease of 15-26% across Colorado headwater basins. These drier spring conditions bring about fewer clouds and result in warmer temperatures. Spring temperatures are better correlated with spring precipitation than with the temporal temperature trend associated with global warming. The greater radiation at the surface from cloud-free skies increases evaporative water losses, particularly in areas where snow has recently disappeared, leading to lower surface albedo and more net radiation available for evapotranspiration. Lower elevation

headwater basins, where snowmelt occurs earlier, experienced the most substantial annual streamflow decreases of up to 41%. Refining spring precipitation estimates will be imperative for future water availability forecasts in snow-dominated water resource regions throughout the world.

Introduction

The Upper Colorado River Basin (UCRB) (Fig. 1*A*) constitutes approximately 90% of the total flow of the Colorado River (Lukas & Payton, 2020; McCabe & Wolock, 2007; Xiao et al., 2018), one of the most over-allocated water resource regions in the world (Christensen et al., 2004; Fleck & Udall, 2021; Vano, 2020). Annual streamflow at the outlet of the UCRB has decreased by 19% (*SI Appendix,* Table S2) during the ongoing Millennium Drought ("MD") (2000-2023), relative to both the historical record (1906-1999) and the baseline period used in this analysis (1964-1999). The winter snowpack, originating in the headwater regions of the basin, is the most critical component to streamflow in the UCRB (Christensen et al., 2004; Li et al., 2017; Palmer, 1988). Given the relative importance of snow to streamflow (Q), 1 April snow water equivalent (SWE) is commonly used as a vital predictor for operational seasonal streamflow forecasts (Mahanama et al., 2012; Pagano et al., 2014). However, between the MD and

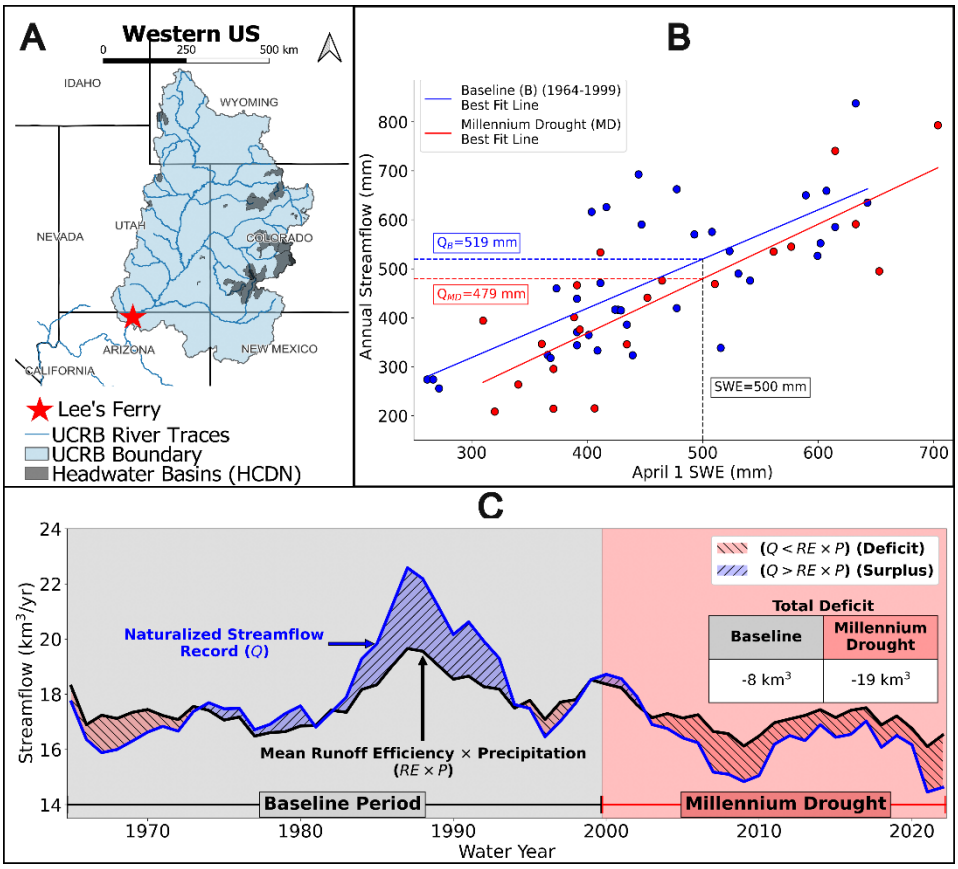

Fig. 1. *(A) Map of the UCRB with locations of headwater basins used in this analysis with the outlet at Lee's Ferry (red star). (B) April 1 SWE snow course measurements from 1964 to 2022 within the Black Gore Creek basin, and area-normalized annual streamflow from Black Gore Creek (USGS gage ID 09066000), in mm. Blue dots symbolize years during the baseline period, and red dots signify years during the Millennium Drought. Using the best fit line, the resultant streamflow estimate (Q) was made for each period with 500 mm SWE. Resultant streamflow estimates for the baseline period and Millennium Drought are shown in the blue and red text boxes, respectively. (C) UCRB Naturalized streamflow (blue line) as estimated at Lee's Ferry and mean runoff efficiency (0.15) x precipitation (RE x P) (black line) in km³/year. Blue shading denotes periods when naturalized streamflow surpassed RE x P (surplus), and red shading denotes periods when naturalized streamflow fell below RE x P (deficit). Total deficits during each period are shown in the inset table.*

baseline periods, streamflow has reduced for the same input of SWE in headwater basins (Lapides et al., 2022; McEvoy & Hatchett, 2023; Modi et al., 2022) (Fig. 1*B*).

The reduction in UCRB streamflow during the MD has led to the largest basin-wide water deficit on record (Hoerling et al., 2019; Schmidt et al., 2023; Williams et al., 2022; Xiao et al., 2018) (*SI Appendix*, Fig. S3), yet the precipitation deficit during the same period does not fully account for this historic streamflow decline. To demonstrate this, we use the mean runoff efficiency, the ratio of mean annual streamflow to mean annual precipitation, which is 0.15 in the UCRB (Lukas & Payton, 2020; Vano et al., 2012). This ratio, multiplied by annual precipitation, provides a first approximation of annual streamflow. During the Millennium Drought, the observed streamflow was much less than would be expected from this ratio and the observed precipitation (Fig. 1*C*).

Multiple studies have tried to explain this pattern (Fig. 1), without consensus. Some modeling studies point to the temperature sensitivity of streamflow to warming as the main contributor to streamflow decline (Christensen & Lettenmaier, 2007; Ficklin et al., 2013; McCabe et al., 2017; Udall & Overpeck, 2017; Xiao et al., 2018) due to temperature-driven increases in wintertime sublimation and warm-season evapotranspiration (ET), while others postulated that annual precipitation deficits outweigh the contributions from warming (Hoerling et al., 2019; Woodhouse et al., 2016). The disagreement among these studies is partly attributed to variations in model estimations of precipitation and to inherent model differences in how precipitation is allocated to streamflow, which can diverge widely across models (Vano et al., 2012). Thus, the choice of model can significantly influence how streamflow changes are explained (2019) (further discussion is available in the *SI Appendix,* Supplementary Text S2). To avoid challenges with a single model choice, we focus on observations of precipitation, temperature, and streamflow within a network of 26 unregulated UCRB headwater basins (Slack et al., 1994).

While prior studies focused on annual changes, streamflow sensitivity to precipitation and temperature change is dynamic throughout the year (Lehner et al., 2017), suggesting the seasonality of annual water inputs is a vitally important metric to consider. Here, we specifically focus on the seasonality of precipitation to deduce its impact on annual streamflow. The timing and location of water fluxes in relation to ET play a primary role in mediating streamflow volume (Carroll et al., 2020; Foster et al., 2016; Meira Neto et al., 2020). Furthermore, seasonality strongly influences the energy available to transpire or evaporate water, defined as potential ET (PET) - the maximum amount of water that could be transferred to the atmosphere at a given time. PET is an energy-limited process during cooler months (November-April) and water-limited after the snowmelt season (July-October) (Gordon et al., 2022; Massari et al., 2022). PET increases rapidly as net radiation increases, especially once the highly reflective snow cover melts and disappears (*SI Appendix*, Fig. S9). Actual ET (AET) increases once sufficient water and energy are available and plants are ready to transpire. In the mountains, AET is closest to PET in the spring because sufficient water is available from recently melting snow (*SI Appendix*, Fig. S9).

Spring (April – June) marks a rapid transition in snow-dominated headwater regions. As streamflow responds to snowmelt, the annual phenological cycle begins, PET rises rapidly, and precipitation transitions from snow to rain. With these changes, spring precipitation is critically important to streamflow in the UCRB, as it exhibits a stronger correlation with annual streamflow than winter precipitation does (S. Zhao et al., 2023) *SI Appendix*, Fig. S7). Observations have shown a decreasing trend in spring precipitation over the last century (Kalra & Ahmad, 2011), but research has not focused on spring precipitation changes during the MD as a driver for

UCRB streamflow declines. Previous work has indicated spring precipitation will decrease west of the Rocky Mountains during the 21st century (McAfee & Russell, 2008), due to a northeastward shift in storm tracks (Yin, 2005) and changes in large-scale climate signals (R. Miller et al., 2006). We hypothesize that spring precipitation has decreased significantly during the MD compared to the baseline in UCRB headwater basins and over the UCRB as a whole. We expect these decreases to constitute the largest portion of annual precipitation deficits when compared to other seasons. To evaluate this, we examined both gridded precipitation products (PRISM Climate Group, 2014) and point gauge observations (National Centers for Environmental Information., n.d.).

Drier and warmer springs shift the timing of plant growth earlier (Cayan et al., 2001; Schwartz & Reiter, 2000), while decreases in precipitation (and its associated cloud cover) increase mean temperature (W. Zhao & Khalil, 1993) and radiative input (Betts et al., 2014), all important contributors to ET (Betts et al., 2014; Sumargo & Cayan, 2018). Thus, years with lower spring precipitation correspond to those with higher spring PET, due to warmer temperatures and higher radiative input associated with the decreased precipitation. The impacts from reduced spring precipitation and higher spring PET during drier springs should not impact all headwater basins equally. Snow in lower elevation headwater basins melts out earlier (Fassnacht et al., 2003; Lundquist et al., 2004). Two main consequences from this earlier snowmelt impact spring PET over lower, but not higher, elevation basins: (1) surface albedo decreases earlier, significantly increasing the radiative input into the surface, and (2) plant-driven ET starts earlier. Here, we use stream gage records from the same headwater basins, which account for 24% of UCRB streamflow, separated into lower (<2900 m), middle (2900-3200 m), and higher (>3200 m) elevation groups to test our second hypothesis: annual streamflow volume in lower (<2900 m) elevation headwater basins is disproportionately impacted by reduced spring precipitation and higher spring PET during drier springs during the Millennium Drought.

Results

Spring Precipitation Decreases Between Periods

Over the entire UCRB, there was a statistically significant ($P = 0.04$) reduction in annual precipitation of 7% between the Millennium Drought and the baseline periods (*SI Appendix,* Fig. S3, and Table S2). Concentrating on the headwater basins, 17 of 26 basins show significant ($P < 0.05$) decreases in annual precipitation (*SI Appendix*, Table S2). Most of these significant changes were concentrated in the lower and middle elevation basins below 3200 meters. Seven of the 11 precipitation gages showed significant decreases in annual precipitation (Fig. 2*B*), consistent with the streamflow shifts seen in the corresponding basins (*SI Appendix*, Table S2).

Widespread reductions in spring precipitation were evident throughout the UCRB (Fig. 2*B*), which exhibited a significant ($P = 0.01$) 17% decrease in spring precipitation between periods (*SI Appendix*, Table S2). All headwater basins studied in this analysis showed at least a marginal decrease in spring precipitation between periods (*SI Appendix*, Table S2), while 15 of the 26 headwater basins registered significant ($P < 0.05$) decreases. Similar to the annual precipitation declines, lower and middle elevation basins below 3200 meters were the focal point for these declines, as 12 of 16 basins showed significant decreases (*SI Appendix*, Table S2). In line with these findings, all precipitation gages recorded decreases between periods, while significant ($P < 0.05$) reductions in spring precipitation occurred at nine of 11 gages (Fig. 2*B*).

At both the headwater basin and UCRB scales, spring precipitation decreases between the baseline and the MD accounted for the largest portion of the annual precipitation deficit. In 16 of the 17 basins with significant decreases in annual precipitation between periods, spring

precipitation reductions accounted for the bulk (31-51%) of the annual deficit (*SI Appendix*, Fig. S8). Over the entire UCRB, the spring precipitation deficit accounted for the largest portion (43%) of the annual deficit, compared to the other seasons. We observed limited changes in fall, winter, and summer precipitation between periods throughout both the UCRB and the headwater basins (Fig. 2*B*). A more detailed discussion of these changes and the weak relationship between precipitation across seasons is available in the *SI Appendix* Supplementary Text S4.

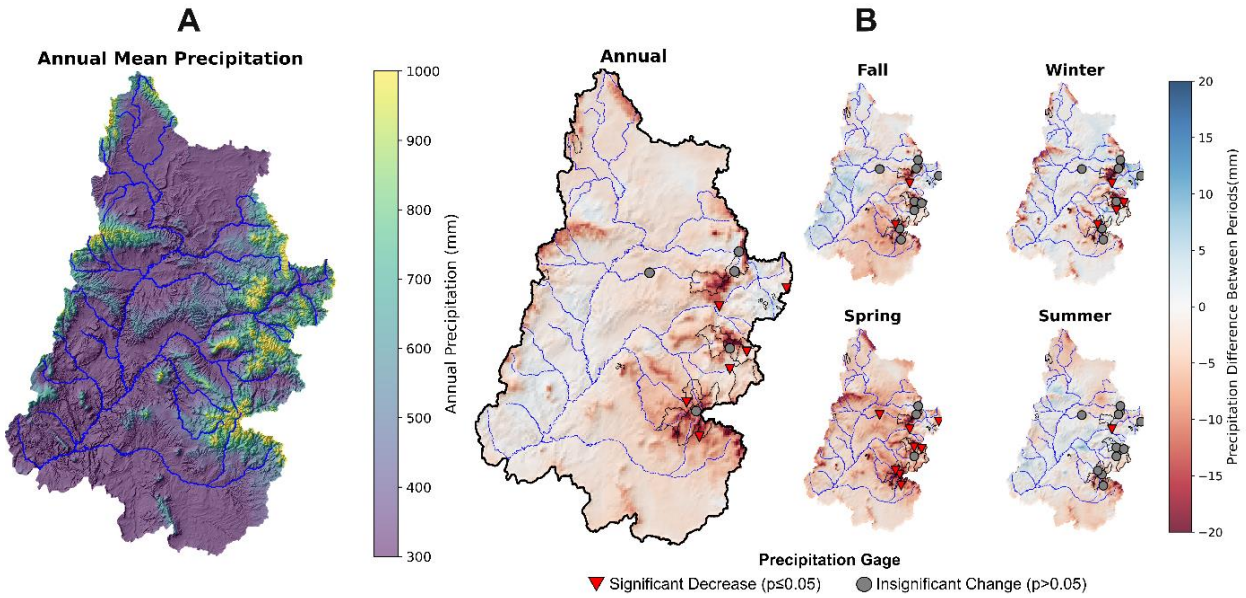

Fig. 2. *(A) Climatological average (1991-2020) precipitation from PRISM over the UCRB. (B) Annual and seasonal precipitation difference between the Millennium Drought and the baseline periods. Colors indicate the magnitude of the difference in millimeters. Precipitation gages used for PRISM validation are also shown with significant decreases (downward red arrow) or insignificant (grey circle) changes in annual or seasonal precipitation between periods.*

Streamflow Volume Decrease Differs by Headwater Basin Elevation

We found years with less spring precipitation had amplified spring evaporative losses in the UCRB. With a median Pearson's correlation of -0.5 (±0.13), spring precipitation negatively correlated with spring PET (for further details see *SI Appendix*, Supplementary Text S4, and Fig S5). Additionally, the spring precipitation-temperature relationship was stronger than the increasing temporal trend in spring temperature attributed to global warming (*SI Appendix*, Supplementary Text Fig. S11). Since ET increases more rapidly over bare soil compared to snow (Hutchison, 1966), we separated basins by elevation groups to examine whether the spring precipitation-PET relationship compounded streamflow reductions differently for lower basins with earlier snowmelt compared to higher basins with later snowmelt (Fig. 3). Reductions in annual streamflow were significant ($P < 0.05$) in two of the 10 higher elevation basins (>3200 m) (*SI Appendix*, Table S3), with reductions between -10 and -19%. In the middle and lower elevation basins (<3200 m), 13 of 16 basins showed significant ($P < 0.05$) decreases in annual streamflow, ranging between -12 and -41%. The largest changes occurred in the lowest elevation group (Fig. 3, *SI Appendix*, Table S3).

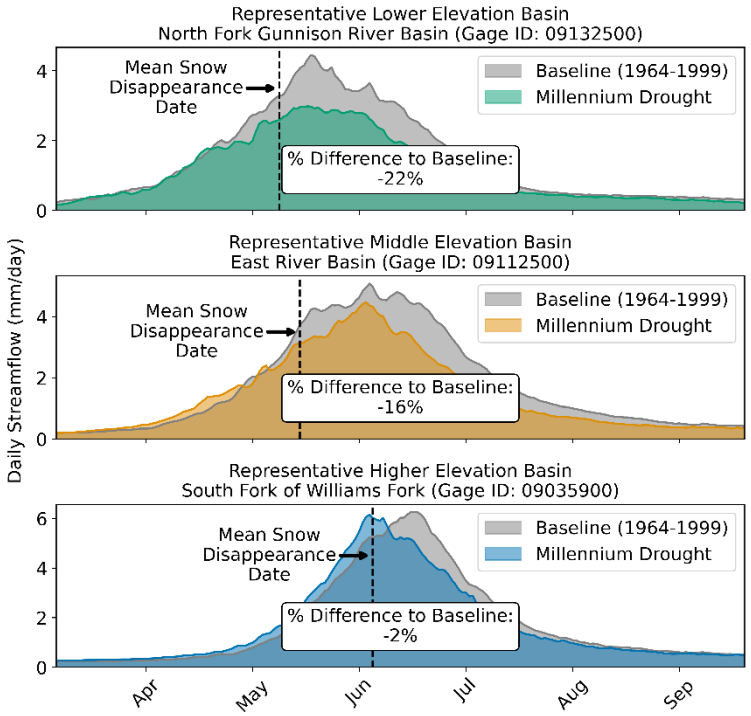

Fig. 3. *Basin normalized daily streamflow averaged over water years within the baseline (gray) and Millennium Drought (colored) periods in mm/day for a representative lower, middle, and higher elevation basin. Basin locations are marked in Fig 4A. The percent changes of streamflow volume relative to the baseline are expressed in the text boxes. The mean snow disappearance date, derived from MODIS snow covered area data between 2000-2018 (O'Leary et al., 2020), is the date when 50% of each basin's snow covered area has disappeared, More details are available in the SI Appendix, Supplementary Text S4. Note the earlier timing at lower elevations.*

Discussion

Springtime precipitation decreases served as a major signal of reduced water input across the UCRB headwater regions and the greater basin area. Between the baseline and MD periods, spring was the only season with a significant reduction in seasonal precipitation, aligning with the significant annual precipitation reduction (Fig. 2*B*, *SI Appendix*, Table S2). These spring precipitation deficits dominated annual precipitation deficits in both the headwater basins and the entire UCRB during the MD (*SI Appendix*, Fig. S8). While spring precipitation decreased throughout all headwater basins, the largest decreases were centered in the lower and middle elevations (*SI Appendix*, Table S2).

These spring precipitation decreases corresponded with decreases in annual streamflow (Fig. 4*B*), implying the reduction in spring precipitation during the MD is a vital contributor to these streamflow deficits. Nonetheless, these decreases alone do not fully account for the observed UCRB streamflow deficits (Fig. 1*B*). To address this incongruity and delve further into the consequences of reduced spring precipitation, we showed that springs with less precipitation incur greater PET, leading to increased surface water losses during this crucial season. Across the UCRB, we found a robust negative correlation between spring precipitation and spring PET, indicating drier springs exhibited more PET and warmer temperatures (*SI Appendix*, Fig. S5). However, these warmer temperatures were not simply due to the global warming signal, since the spring precipitation-temperature relationship was stronger than the temporal increasing trend in spring temperature (*SI Appendix*, Fig. S11). With less spring

precipitation, less cloud cover is observed, increasing solar radiation at the surface. This greater solar radiation increases temperatures and energy for PET (Betts et al., 2014; W. Zhao & Khalil, 1993).

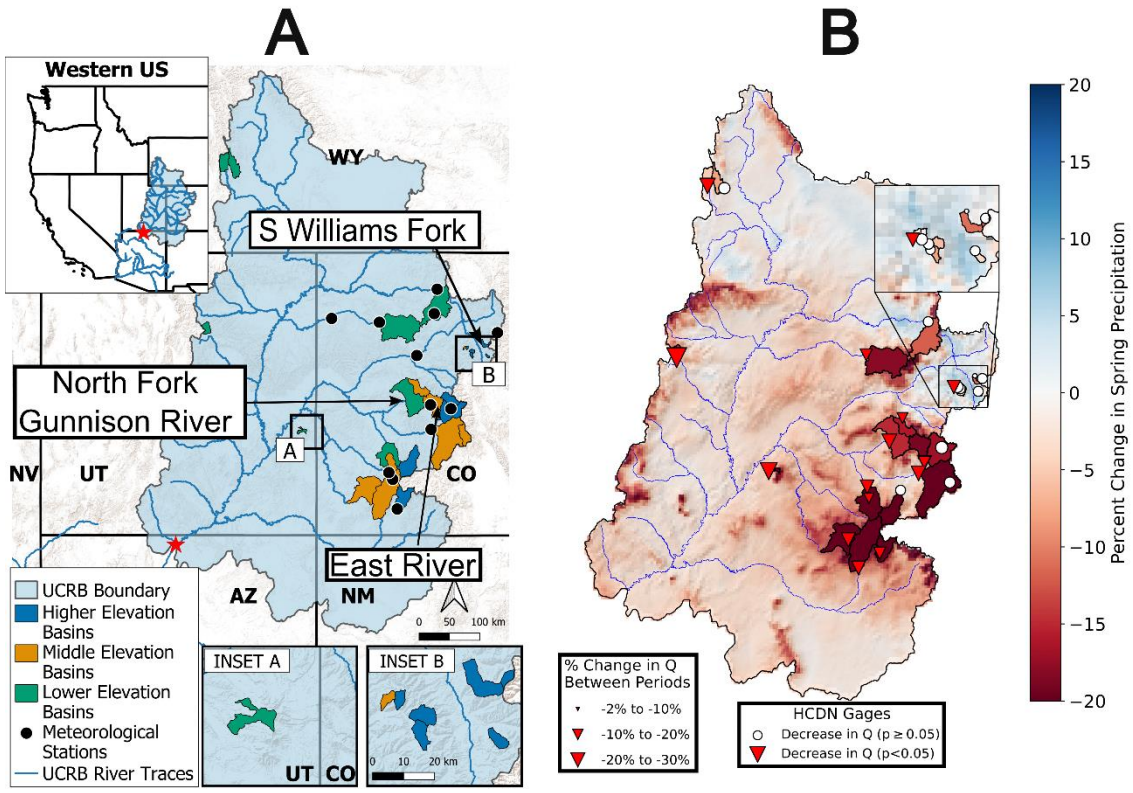

Fig. 4. *(A) Map of UCRB boundary with higher, middle, and lower elevation HCDN basin groupings. Basins depicted in Fig. 3. are pointed out by arrows. (B) Percent change in spring precipitation (shading) and annual streamflow volume (symbols) between baseline and Millennium Drought. Larger downward triangles indicate a larger decrease in streamflow volume, and the color describes the significance level of the change.*

Significant ($P < 0.05$) spring precipitation decreases were concentrated in lower and middle elevation basins (*SI Appendix*, Table S2), and streamflow change during the MD revealed lower and middle elevation basins also exhibited more significant ($P < 0.05$) decreases in annual streamflow volume compared to higher elevation basins (Fig. 3, Fig. 4*B*). The dual impact of less spring precipitation and amplified spring PET is exacerbated by earlier snowmelt in these lower elevation basins. In these lower elevation basins, the timing of the seasonal ET increase occurs earlier due to earlier snowmelt timing from warmer temperatures (Fassnacht et al., 2003; Lundquist et al., 2004). This earlier snowmelt timing increases the energy available at the surface and magnifies the spring PET increase from less spring precipitation (*SI Appendix*, Figs. S5 and S9). Spring is unique in this arid region because it is the only season when recent snowmelt and water availability let AET approach PET, keeping evaporation rates high. In winter, there are instances when AET matches PET, but with limited energy available, overall AET remains low. In summer and fall, even with sufficient energy, drier conditions constrain AET. Given this relationship, the combined effect of spring precipitation decreases and PET increases have a more direct impact on water availability than in other seasons, especially at lower elevations without long-lasting snow cover.

Higher elevation basins above 3200 m showed more modest reductions in annual streamflow volume (*SI Appendix,* Table S3). These basins are less sensitive due to their deeper snowpacks, which not only cover plants but also act to limit the energy available for ET and buffer against the negative spring precipitation-PET relationship. Higher elevation basins may lose this buffering effect if both winter and spring precipitation decrease significantly, resulting in diminished snowpacks at higher elevations. In addition, as temperatures continue to rise, snowmelt is predicted to occur earlier at all elevations (Clow, 2010; Fritze et al., 2011; Modi et al., 2022), further weakening this buffering capacity. In years with small snowpacks, low spring precipitation, and rapid or early spring snowmelt (McEvoy & Hatchett, 2023), streamflow volume within these basins would decrease further.

We demonstrated a strong negative correlation between spring precipitation and PET in the UCRB. However, our analysis did not directly consider AET observations. While studying the spring period allows us to assume AET= PET, future investigations should focus on conducting a more comprehensive analysis of the relationship between springtime precipitation and spring AET and the impacts each exerts on basin hydrology.

Our work highlights the importance of spring precipitation to UCRB streamflow, and further work should be devoted to exploring the underlying causes, such as larger-scale atmospheric and oceanic drivers, of these precipitation reductions. Recent research has used oceanic teleconnections, specifically North Pacific sea surface temperature, to predict spring precipitation and streamflow in the UCRB with encouraging results (S. Zhao et al., 2021, 2023). A better forecast of spring precipitation would benefit water managers in the UCRB region since the inclusion of spring precipitation in forecast models can improve streamflow forecasts (Lehner et al., 2017; S. Zhao et al., 2023) (*SI Appendix*, Fig. S10).

Conclusion

Since the onset of the Millennium Drought in the UCRB, annual precipitation and 1 April SWE have provided less streamflow than historically observed. By highlighting the importance of seasonality, we focused on changes specifically during the spring season to explain the observed inconsistency between SWE, precipitation, and annual streamflow declines in the UCRB during the Millennium Drought. Our analysis revealed significant spring precipitation decreases in headwater regions between the baseline (1964-1999) and the Millennium Drought periods, and spring precipitation decreases notably outweighed precipitation decreases in other seasons. We found that years with less spring precipitation corresponded with greater spring PET and warmer spring temperatures. The relationship between spring temperature and precipitation was stronger than the observed increasing trend in temperature related to global warming. The compounding impacts of springtime precipitation reductions and PET increases associated with these reductions impacted lower elevation basins most, with more significant reductions in annual streamflow volumes observed in these basins than at higher altitudes.

With the continued projections of increasing temperature and reduced precipitation during spring, it will be paramount to highlight the importance of springtime conditions throughout the UCRB and better resolve our estimates of spring precipitation when forecasting water availability. Further work should be undertaken to enhance our understanding of precipitation changes during spring in mountainous headwater regions and focus on the interplay between precipitation and other hydrologic fluxes during this dynamic season.

Data and Methods

Study Basins

Twenty-six headwater basins distributed throughout the UCRB were used in this analysis to define the headwater regions (Fig. 4*A*, *SI Appendix* Table S1). Basins were selected from the USGS Hydro-Climatic Data Network (HCDN), a data set created for the study of hydrologic conditions in natural streams to highlight climatic influences on flow unimpeded by diversions, storage, or other water control structures (Slack et al., 1994). To span the period where all basins had continuous daily streamflow observations, we limited the streamflow data to span all water years in our period of analysis between 1964 and 2022. Daily streamflow data were obtained from the USGS National Water Information System. For each gage, each water year's streamflow volume was calculated from the sum of daily streamflow divided by basin area and converted to millimeters depth.

Basin elevation best characterized different hydrologic responses in each basin in terms of both center-of-mass timing and streamflow volume (*SI Appendix*, Supplementary Text S4, and Table S1). We calculated the area-normalized mean basin elevation for each HCDN basin using the 1-arc second (approximately 30-meter) 3DEP digital elevation model accessed through the USGS National Map. Basins were separated into higher (>3200 m), middle (2900 to 3200 m), and lower (<2900 m) elevation groupings based on their area-normalized mean elevation (Fig. 4*A*). The ten high-elevation basins generally sustained higher area-normalized streamflow and received more annual precipitation than the eight lower elevation basins (*SI Appendix*, Table S1), with the eight mid-elevation basins falling in between (*SI Appendix*, Fig. S6*B*).

Seasonal Precipitation Changes

Monthly precipitation data were collected from the Parameter-elevation Regressions on Independent Slopes Model (PRISM) dataset at 4 km resolution for the 1964-2022 period over the UCRB (PRISM Climate Group, 2014). Additional information about PRISM is available in *SI Appendix* Supplementary Text S3. The monthly precipitation product was spatially averaged over each HCDN basin and the entire UCRB. Seasonal and annual aggregates of precipitation were created for each basin for each water year in the data record. Seasons were delineated as follows to align with the climatology of the UCRB headwaters region (*SI Appendix,* Supplementary Text S1): fall spans October 1 to December 31, winter spans January 1 to March 31, spring spans April 1 to June 31, and summer spans July 1 to September 30.

One caveat of using PRISM, especially with a more extended time series, is that the data are not temporally homogenous, meaning the addition of new stations over time can impact the resulting product (Henn et al., 2018). Nevertheless, prior work tested the homogeneity of PRISM alongside two commonly used gridded precipitation datasets over the UCRB and found PRISM to be the most reliable during the more data-sparse period spanning 1950-1999 (2010). We compared PRISM against 11 precipitation gages in the UCRB headwaters region for the 1964-2022 period (*SI Appendix,* Table S4). Daily precipitation data from these gages were acquired from the National Center for Environmental Information Climate Data Online service and aggregated to seasonal totals. Seven of the 11 stations were located within the boundary of basins used in this analysis, while the remaining four stations were distributed throughout the eastern portions of the UCRB (Fig. 4*A*).

To compare annual and seasonal precipitation changes between periods within the 26 headwater basins and the UCRB, we separated the seasonal precipitation totals into baseline (1964-1999) and MD (2000-2022) periods. We employed Student's *t*-tests (*t*-tests), which require normally distributed data, to compare means between these two groups, and used the

Kolmogorov-Smirnov test to verify normality. We utilized one-sided *t*-tests to assess significant reductions in mean seasonal precipitation between periods in each basin. In these tests, the null hypothesis of no change in the mean was rejected when the probability value (*P* value) of the test statistic was determined to be less than the chosen significance level $\alpha = 0.05$.

Spring Precipitation and PET Relationship

To assess the spring precipitation-PET relationship over the UCRB, we estimated monthly PET values at each grid-cell from 4 km PRISM monthly mean temperatures between 1964 and 2022 using the Thornthwaite equation (Thornthwaite & Holzman, 1939), which has been shown to provide a superior estimate of PET over the UCRB compared to other common empirical methods (Yates & Strzepek, 1994). From these monthly estimates, we calculated spring PET totals for each year. We computed Pearson's correlations (*r* values) between spring PET and spring precipitation at each grid cell. In so doing, we produced a UCRB-wide correlation map between spring PET and spring precipitation over the UCRB (*SI Appendix,* Fig. S5). We then computed the median and standard deviation of the UCRB *r* values derived from total spring precipitation and total spring PET estimates from PRISM. A comparison with other PET estimates is available in the *SI Appendix,* Supplementary Text S4, with similar results.

Streamflow changes between periods by elevation group

We calculated annual streamflow totals from the USGS gages at the outlet of each HCDN basin. To capture a water year estimate of streamflow from the entire UCRB, we used the US Bureau of Reclamation naturalized streamflow record at Lee's Ferry, AZ for water years 1964 to 2022 (2020-2022 data is currently provisional), which is calculated from modeled unregulated flows into Lake Powell from the Colorado Basin River Forecasting Center. The product has been used in several model evaluation and water balance studies as an annual streamflow estimate from the UCRB (Hoerling et al., 2019; Vano et al., 2012; Xiao et al., 2018).

To compare changes in streamflow volume between periods at the 26 headwater gages, we separated annual streamflow totals into baseline and MD periods. Since not all basins had normal distributions in their annual streamflow time series, we used the one-sided Wilcoxon rank sum test to assess significant decreases in the mean annual streamflow between periods. In these tests, the null hypothesis of no change in the mean was rejected when the probability value (*P* value) of the test statistic was evaluated to be less than the given significance level $\alpha = 0.05$. We then bundled each basin's result into its elevation grouping and compared test results between these groupings.

Data Availability

Previously published data were used for this work. All data are publicly available, and sources are provided in *SI Appendix,* Table S5.

Acknowledgements

We gratefully acknowledge funding support for this analysis from the National Science Foundation (Award No. 2139836), Sublimation of Snow, and from the Department of Energy Environmental System Science Division (Award No, DE-SC0024075), Seasonal Cycles Unravel Mysteries of Missing Mountain Water. Additionally, we thank all members of the Sublimation of Snow project and the Mountain Hydrology Research Group at the University of Washington for their valuable feedback and insight. The author would also like to offer a sincere thank you to his advisor, Jessica Lundquist, for her continuous insight, guidance, and mentorship in this area of study. Additionally, the author would like to thank his family and the unending support from his partner, Grace Miles, and dog, Denali.

Supplementary Information (SI) Appendix

Supplementary Text S1: The Climatology of the Upper Colorado River Basin

The UCRB, defined as the drainage area of the Colorado River upstream of the Lee's Ferry gaging station (USGS station 09380000) (Fig. S1), contributes approximately 90% of the total flow of the CRB (Lukas & Payton, 2020; McCabe & Wolock, 2007; Xiao et al., 2018). An estimated 70-90% of this streamflow originates in the headwater basins of the UCRB (Christensen et al., 2004; Li et al., 2017; Palmer, 1988).

The UCRB can be characterized as a region of contrast and diversity in its terrain and ecology. Most of the area within the UCRB is classified as arid or semi-arid, meaning less than 500 millimeters of precipitation falls over it each year (Fig. S2*A*). These semi-arid areas contribute substantially less runoff to the region's rivers than the high-elevation basins, where complex topography enhances precipitation through orographic processes. In the intermediate zones between arid and alpine regions, strong gradients in temperature (Fig. S1*B*) and precipitation (Fig. S2*A*) support a wide range of vegetation zones. Forest cover closely aligns with regions of greater precipitation (Figs. S1 and S2), except for the uppermost reaches of the basin, which experience a harsher environment characterized by colder temperatures and shorter growing seasons, restricting tree growth.

Spatial precipitation patterns, while driven by singular storm systems throughout the year and influenced by topography and elevation, are derived from large-scale atmospheric dynamics with distinct seasonal moisture sources and trajectories. These seasonal differences lead to seasonality in precipitation (Fig. S2 *B* through *E*) and streamflow that influence regions differently throughout the UCRB. Seasonal precipitation in higher-elevation basins is skewed towards the winter and spring months; however, in lower-elevation basins, precipitation is more equally distributed across the year (Lukas & Payton, 2020).

We used seasonal means of PRISM precipitation between 1964 and 2022 to compare the distribution of precipitation over the year in the headwater basins of the UCRB that we analyzed. Winter precipitation (January through March) makes up around 29% of annual precipitation (Fig. S2*B*). Snow cover and low solar angles limit the amount of energy available evapotranspiration (ET), the combined process of water vapor transfer into the atmosphere through evaporation from surfaces and plant transpiration, is minimized. With much of the water in the UCRB frozen within the snowpack, streamflow remains low until snowmelt begins. Spring precipitation (April through June) constitutes 28% of annual precipitation (Fig. S2*C*). Spring also coincides with the startup of plant activity and increases in ET as snow cover decreases and solar energy increases. The onset of snowmelt and continued spring precipitation lead to the peak in the annual hydrograph late in spring or early in summer. Summer precipitation represents approximately 22% of annual precipitation (Fig. S2*D*). Summer contains the peak ET rates during the year, due to the high temperatures driving large water vapor gradients and peak solar energy needed to power evaporation and plant growth. Streamflow response to summer precipitation is limited due to plants' substantial influence on water partitioning to ET rather than runoff (Sprenger et al., 2022). Fall precipitation makes up 21% of annual precipitation (Fig. S2*E*). As plants senesce for the winter, so does the amount of ET as the region returns to winter conditions. With few significant precipitation events early in the fall, minimum annual flows that are driven by baseflow from groundwater stored within each basin usually occur during this time.

Supplementary Text S2: Additional Background Information

Contextualizing the Millennium Drought in the UCRB

The Millennium Drought has been characterized by 20% less annual naturalized streamflow at Lee's Ferry compared to the earlier historical record spanning 1906-1999 (Udall & Overpeck, 2017). Reconstructions of even longer historical CRB streamflow from tree-ring analysis further contextualized the extreme nature of the current low-flow state within the UCRB. Although currently shorter in duration, the ongoing Millennium Drought is similar in magnitude to some of the most severe multi-decadal drought periods in the past several centuries (Gangopadhyay et al., 2022; Gray et al., 2011; McCabe & Wolock, 2007; Salehabadi et al., 2022). Relative to the baseline period (1964-1999), the mean streamflow deficit during the Millennium Drought was 3.35 km^3 per year or a 19% difference between the baseline and the Millennium Drought (Fig. S3*A*). Concurrent with this change, precipitation decreased by 7% between periods (as estimated by PRISM) (Table S2), amounting to a mean annual deficit of 8.31 km^3 per year (Fig. S3*B*). The UCRB exhibits a mean runoff efficiency of around 0.15 (Lukas & Payton, 2020; Vano et al., 2012), indicating that the precipitation decrease would need to be more than doubled to match the observed streamflow deficit, presuming this efficiency is constant in time (main text, Figure 1*C)*. Thus, observations suggest that each unit of precipitation is no longer providing the same amount of streamflow since the onset of the Millennium Drought.

Numerous future scenarios and historic modeling efforts have studied how recent warming and precipitation changes (Figs. S3*A* and S3*B*) have impacted UCRB flows to explain this decrease in runoff and precipitation-streamflow discrepancy, without consensus (Bass et al., 2023; Christensen et al., 2004; Christensen & Lettenmaier, 2007; Ficklin et al., 2013; Hoerling et al., 2019; McCabe et al., 2017; McCabe & Wolock, 2007, 2011; Udall & Overpeck, 2017; Vano et al., 2012, 2014; Woodhouse et al., 2016; Xiao et al., 2018). Many of these investigations have contextualized the individual impact that precipitation change and temperature increase have on streamflow using land surface models (LSMs) (Bass et al., 2023; Christensen et al., 2004; Hoerling et al., 2019; McCabe & Wolock, 2007; Udall & Overpeck, 2017; Vano et al., 2012, 2014; Xiao et al., 2018). These investigations separated the influences that precipitation and temperature change have on Colorado River flow by estimating streamflow temperature sensitivity and precipitation elasticity.

Temperature sensitivity can be defined as the percent change in streamflow due to a 1º C increase in temperature. Models indicate temperature sensitivities of UCRB streamflow range between -3% to -10% per 1º C increase (Bass et al., 2023; Hoerling et al., 2019; McCabe et al., 2017; McCabe & Wolock, 2007; Udall & Overpeck, 2017; Vano et al., 2012; Vano & Lettenmaier, 2014). Precipitation elasticity is the sensitivity of streamflow to a 1% change (positive or negative) in precipitation. UCRB precipitation elasticities typically range between 1.8 and 4, but uncertainties are largely driven by the choice of LSM, and values can vary widely across the UCRB (Vano et al., 2012; Vano & Lettenmaier, 2014). However, relationships between these two metrics have been identified that can influence their values during drought periods. Vano & Lettenmaier (2014) found larger decreases in precipitation lead to reduced precipitation elasticity, implying that temperature sensitivity may play a greater role during warmer, dry conditions. This idea was supported by Woodhouse and Pedersen (2018), who found warm temperatures during persistent drought conditions exacerbate streamflow declines beyond what would be expected solely from precipitation deficits.

Some modeling studies found rising temperatures to be the leading cause for the recent UCRB streamflow decline, and the streamflow decline was largely explained by temperature-driven increases in wintertime sublimation and warm-season ET (Bass et al., 2023; Christensen & Lettenmaier, 2007; Ficklin et al., 2013; McCabe et al., 2017; Xiao et al., 2018). Model output

from these studies showed minimal change in annual precipitation (+1% to -3%) since 2000 relative to the long-term mean.

On the other hand, other modeling studies attributed the greatest portion of streamflow change to precipitation decreases (Hoerling et al., 2019; McCabe & Wolock, 2011; Udall & Overpeck, 2017; Woodhouse et al., 2016), with decreases ranging between -4 to -7% since 2000. For example, Hoerling et al. (2019) and Woodhouse et al. (2016) each used different model setups to show precipitation decreases contributed to approximately 60-80% of the reduced UCRB flows during the Millennium Drought, with temperature rise being a secondary factor. McCabe & Wolock (2011) showed that precipitation accounted for almost all variability in streamflow throughout water resource regions of the U.S., including the UCRB, over the past century. Udall & Overpeck (2017) attributed approximately 70% of streamflow change to decreases in precipitation during the Millennium Drought.

These studies disagree on whether decreased precipitation or increased temperatures have controlled UCRB streamflow decline during the Millennium drought, but the distinguishing difference in these findings appears to stem from how precipitation and temperature changes are estimated by different models and how each model translates precipitation into streamflow. Vano et al. (2012) demonstrated that commonly used LSMs diverge widely in determining how precipitation and temperature changes impact streamflow, due to different precipitation elasticities and temperature sensitivities between the LSMs. Bennet et al. (2019) also found stark variations in how water balance variables are treated across models. Thus, the choice of LSM can significantly influence how these changes impact modeled streamflow. In this analysis, we sought to avoid these potential issues associated with model choice by centering our analysis on observations of streamflow and precipitation throughout the UCRB during a period when we have reliable estimates for each.

The Importance of Seasonality within the UCRB Headwater Regions

Despite the focus on changes in precipitation and temperature since the onset of the Millennium Drought, few modeling or observational analyses have centered on when these changes have occurred on an intra-annual scale, particularly precipitation. The importance of seasonal precipitation in the UCRB region was underscored by Fatichi et al. (2012), who showed regions with large inter-annual variability in precipitation, like the UCRB, also have large intra-annual variability in the seasonal precipitation signal. While results from Woodhouse et al. (2016), McCabe et al. (2017), and Xiao et al. (2018) both differentiated intra-annual changes in the UCRB, they each limited their analysis to only cool (October to March) and warm (April to September) season precipitation signals. Recent research has also emphasized the importance of precipitation seasonality and its impact on streamflow in headwater regions. For instance, a modeling study focusing on a headwater basin of the UCRB from Carroll et al. (2020) found that summer rain produced half the amount of runoff as spring snow for the same input of precipitation due to the relative increase in ET between spring and summer within the lower elevation forests of the basin.

Furthermore, attention in these historical investigations, either driven by models or observations, has generally been limited to changes in flow estimates over the entire UCRB, rather than focusing on the hydrologically impactful and sensitive headwater basins. It is in these basins that research has identified shifts towards earlier spring runoff timing (Cayan et al., 2001; Clow, 2010; Heldmyer et al., 2022; Pribulick et al., 2016; Stewart et al., 2005; Tennant et al., 2015), driven by the earlier onset of snow melt due to warmer temperatures in recent decades (Barnhart et al., 2016; Clow, 2010; Fritze et al., 2011; McCabe & Clark, 2005; Modi et al., 2022). However, headwater basins do not respond equally to these changes: lower elevation basins that lie near the early-spring snow line, approximately 2500-3000 meters in the

UCRB (Moore, 2012), have been more broadly impacted (Bohr & Aguado, 2001; Knowles & Cayan, 2004; Mayer & Naman, 2011; Mote, 2006; Tennant et al., 2015; Van Kirk & Naman, 2008). Thus, basin elevation has been identified as a primary driver for how a basin responds to temperature, precipitation, or land cover change (Biederman et al., 2022; Carroll et al., 2019; Foster et al., 2016; Mayer & Naman, 2011; Tennant et al., 2015), underscoring the importance of focusing on a variety of headwater basins when attempting to determine how changing water fluxes impact streamflow more broadly. Additionally, since these basins have reliable, long-term observations of streamflow, we can test hypotheses related to elevational differences in streamflow response that do not need to only rely on model output to evaluate these changes. For example, these observations allow us to determine how spring ET increases might impact streamflow differently in basins with later snowmelt and reduced vegetation cover (i.e., higher elevations) compared to basins with earlier snowmelt and greater vegetation cover (i.e., lower elevations).

Supplementary Text S3: Additional PRISM Details

PRISM Selection

PRISM uses statistical interpolation from point measurements alongside a digital elevation model (DEM) to account for the complex relationships between climate variables and elevation, allowing for more accurate predictions in mountainous regions where traditional linear models may not suffice. PRISM was selected due to its wide use as a spatial climate dataset in hydrologic models (Daly et al., 2008; Lundquist et al., 2015; Raleigh & Lundquist, 2012), including use in several investigations of precipitation and streamflow in the Colorado River basin (Biederman et al., 2022; Brooks et al., 2021; Castle et al., 2014; Clow, 2010; McCabe & Wolock, 2007; M. P. Miller, 2012; Nowak et al., 2012; Udall & Overpeck, 2017; Woodhouse & Pederson, 2018). While PRISM can produce large errors when evaluating precipitation totals for extreme storm events or uncommon storm configurations, its performance improves considerably when considering longer-term climatology where these outliers do not dominate over a longer period (Lundquist et al., 2015), as we do in this study.

Supplementary Text S4: Additional Precipitation, PET, and Snow Analyses and Discussion

Results from Fall, Winter, and Summer Precipitation Changes

Significant decreases in fall precipitation between periods were limited to only three of 26 headwater basins (*SI Appendix*, Table S). Decreases were insignificant ($P > 0.05$) over the UCRB (Fig. 2*B*), although the basin had a moderate 9% reduction in fall precipitation between periods (*SI Appendix*, Table S). Insignificant ($P > 0.05$) decreases in fall precipitation were also seen throughout most of the headwater basins. Only two of the 11 precipitation gages showed significant precipitation decreases (Fig. 2*B*), although 10 of these precipitation gages showed decreases, agreeing with the results from PRISM.

We observed limited change in winter precipitation between periods throughout both the UCRB and the headwater basins (Fig. 2*B*). The entire basin showed an insignificant ($P > 0.05$) 6% decrease in winter precipitation (*SI Appendix*, Table S2). While the largest changes in precipitation between periods were concentrated in the headwater regions, only six of the 26 headwater basins showed a significant ($P < 0.05$) decrease in winter precipitation (*SI Appendix*, Table S2). All other basins showed insignificant ($P > 0.05$) decreases or increases in winter precipitation (*SI Appendix*, Table S). Similarly, four of the 11 precipitation gages distributed throughout the eastern portion of the UCRB showed significant ($P < 0.05$) decreases in winter precipitation (Fig. 2*B*) between -15% and -21%, with the remaining gages showing insignificant ($P > 0.05$) changes between +13% and -11%. This variability across stations generally agreed with the basin-specific analysis from PRISM.

Throughout the UCRB, summer precipitation changes were limited (Fig. 2*B*). A modest 5% decrease in summer precipitation was observed across the UCRB, primarily impacting the northern and eastern reaches of the UCRB (Fig. 2*B*). No headwater basins showed significant ($P < 0.05$) decreases in summer precipitation (*SI Appendix*, Table S). In agreement with these findings from PRISM, only one of the 11 precipitation gages recorded a significant reduction in summer precipitation between periods (Fig. 2*B*).

Evaluation of Seasonal Precipitation Correlations

To distinguish the importance of precipitation seasonality across the UCRB, we evaluated how seasonal precipitation in one season correlated with precipitation in surrounding seasons. We would expect low correlation values if seasonal precipitation anomalies were not similar between seasons, e.g., a relatively wet winter would not imply a relatively wet spring would follow, or that a wet fall preceded it. For each headwater basin we analyzed, we used the basin averaged time series of seasonal precipitation between 1964 and 2022 from PRISM to calculate Spearman's correlation of precipitation between seasons. We found precipitation was not significantly correlated from one season to the next throughout the headwater basins (*SI Appendix*, Fig. S4). Therefore, we found it essential to evaluate how the annual precipitation decreases observed during the Millennium Drought were distributed across the four seasons.

Potential Evapotranspiration Result Comparison

We compared the results from PRISM to monthly gridded PET, temperature, and precipitation estimates from TerraClimate, a climate and water balance dataset that provides global gridded monthly estimates of various climate variables from 1958 to the present at ~4km resolution (Abatzoglou et al., 2018). From these monthly estimates, we calculated spring PET totals for each year. We computed Pearson's correlations (*r* values) between spring PET and spring precipitation at each grid cell to assess the strength of the spring PET-precipitation relationship. In so doing, we produced a UCRB-wide correlation map between spring PET and spring precipitation over the UCRB for both PRISM and TerraClimate data.

Results from the 4-km TerraClimate data and the 4-km PRISM data indicate a negative correlation between spring precipitation and spring PET, with median basin-wide *r* values of 0.72 and 0.50, respectively (Fig. S5). Additionally, years with more significant negative spring temperature anomalies (colder springs) typically coincide with higher springtime precipitation (Fig. S5 *C* and *D*).

Basin Snowmelt Timing Estimate

For each basin shown in Fig. 4 (main text), we estimated the mean snowmelt date with a snowmelt timing product derived from the MODIS snow-cover data from the Terra satellite (Snowmelt Timing Maps Derived from MODIS for North America, Version 2) (O'Leary et al., 2020). This product offers an 18-year time series mean snowmelt date for each 500-m MODIS pixel across North America spanning 2000-2018. This dataset was utilized because it has been shown to have a high degree of agreement with in-situ observations (O'Leary et al., 2018). With this product, we estimated the mean snowmelt date of each basin used in Fig. 4 (main text) by clipping the raster to each basin boundary and calculating the mean snowmelt date from the time series. These basins included the North Fork Gunnison River, the East River, and the South Fork of Williams Fork (Table S1). The mean snowmelt date for the North Fork Gunnison River, the lowest elevation basin of the three, was approximately May 4 with a standard deviation of around 25 days across the basin. The mean snowmelt date for the East River, the middle elevation basin, was approximately May 20, with a standard deviation of around 25 days across the basin. The mean snowmelt date for the South Fork of Williams Fork, the highest elevation basin of the three, was approximately June 10 with a standard deviation of around 14 days across the basin.

Basins Delineation by Elevation

The ten high-elevation basins generally sustained higher area-normalized streamflow and received more annual precipitation than the eight lower-elevation basins (Table S1). The eight mid-elevation basins primarily rested between these groups (Fig. S6B). The USGS gages from these basins, along with station name, area normalized mean elevation, elevation grouping, drainage area size, and mean annual precipitation, are shown in Table S1. We also calculated the timing of the streamflow center of mass (Stewart et al., 2005). Center-of-mass in the higher elevation basins averaged about 9 days later than the middle elevation basins, while the average lower elevation basin center-of-mass timing was approximately 10 days earlier than the middle elevation basins (Table S1).

Areas for Further Research

Our study did not address the roles of soil moisture and groundwater, important contributors to the water balance in headwater basins (Carroll et al., 2018, 2019; Mayer & Naman, 2011; M. P. Miller et al., 2016; Ryken et al., 2020). Nevertheless, it is probable that these reductions in spring precipitation contribute to negative anomalies in fall soil moisture. Such anomalies have been demonstrated to play an important role in converting snow to streamflow(Harpold et al., 2017; Mahanama et al., 2012). To gain deeper insights into these water balance components, further research should be undertaken to examine how water partitions to soil moisture and groundwater during years with anomalously low spring precipitation.

Supplementary Text S5: Data Sources

Data sources and access dates are labeled in Table S5. The UCRB boundary was obtained from https://www.sciencebase.gov/catalog/item/4f4e4a38e4b07f02db61cebb. Basin elevations were calculated from the 30m 3DEP digital elevation model downloaded from the National Map from https://www.usgs.gov/programs/national-geospatial-program/national-map. Fractional tree-covered area estimates were derived from the National Land Cover Dataset with data downloaded from https://www.mrlc.gov/data. UCRB Daily streamflow data from NWIS were downloaded from https://waterdata.usgs.gov/nwis? using the dataretrieval Python package (https://pypi.org/project/dataretrieval/0.1/). The USBR naturalized streamflow record was obtained from https://www.usbr.gov/lc/region/g4000/NaturalFlow/provisional.html. HCDN basins and basin polygons were obtained from https://water.usgs.gov/GIS/metadata/usgswrd/XML/gagesII_Sept2011.xml. PRISM climatological normal and monthly estimates for precipitation and temperature were downloaded from https://prism.oregonstate.edu/. Precipitation data from stations used to validate PRISM results were acquired from the NOAA Climate Data Online portal at https://www.ncdc.noaa.gov/cdo-web/. Snow course and snow pillow SWE measurements were acquired from https://www.nrcs.usda.gov/resources/data-and-reports/snow-and-climate-monitoring-predefined-reports-and-maps using the Metloom python package (https://metloom.readthedocs.io/en/latest/readme.html). Output from a 1987-2020 1 km WRF model run (Rudisill et al., 2022) was downloaded from https://data.ess-dive.lbl.gov/view/doi:10.15485/1845448. Snowmelt timing maps derived from MODIS were downloaded from https://daac.ornl.gov/cgi-bin/dsviewer.pl?ds_id=1712. Monthly TerraClimate data were downloaded from https://www.climatologylab.org/terraclimate.html.

Supplementary Figures

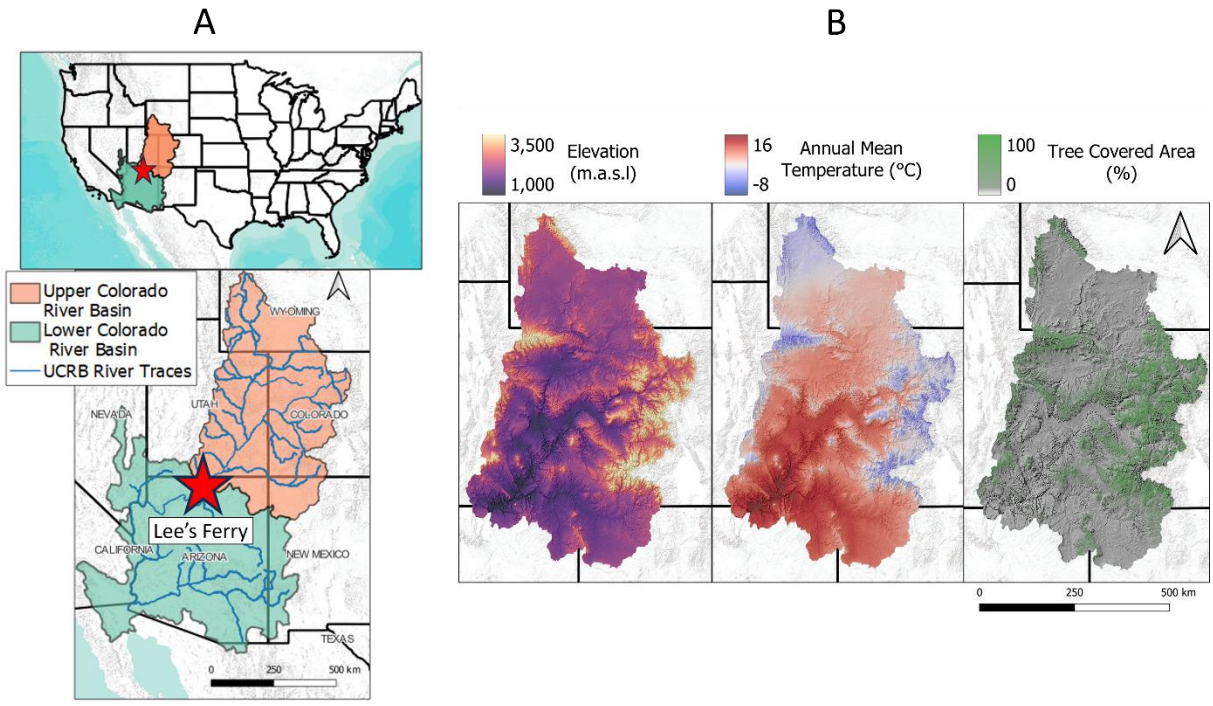

Fig. S1 – *(A) Map of the Upper and Lower Colorado River Basin with trace of major tributaries and the location of Lee's Ferry. (B) UCRB 30-m resolution elevation map from 3DEP, annual mean temperature from PRISM climate normals, and tree covered area from the National Land Cover Dataset (NLCD).*

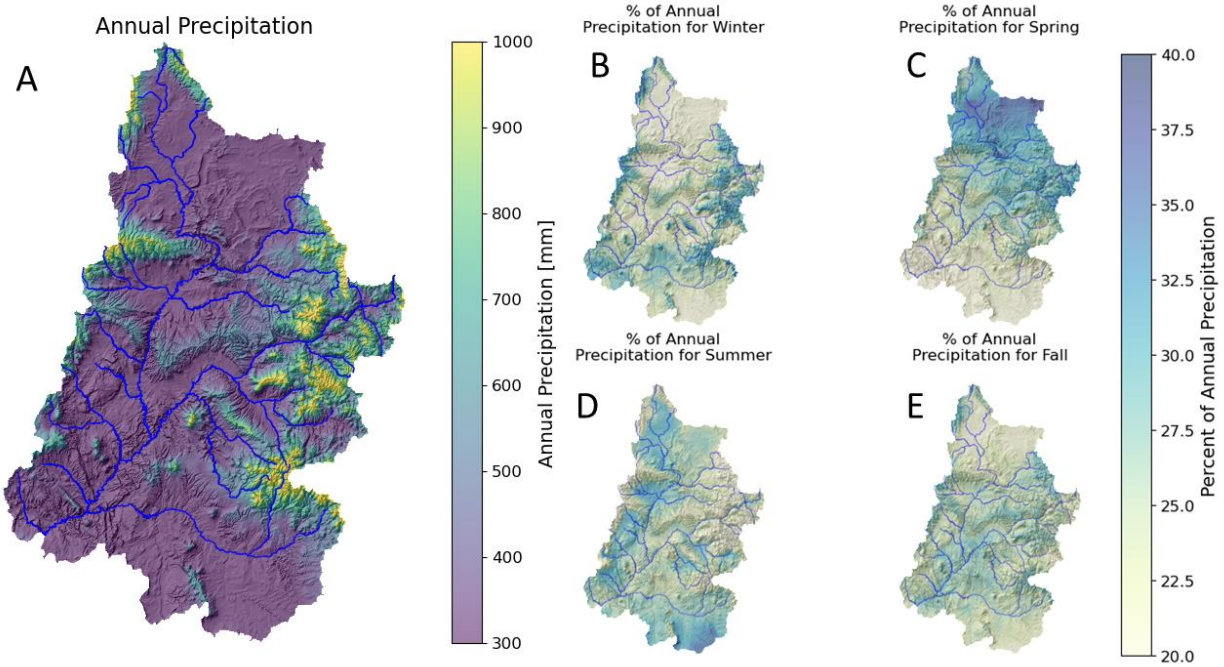

Fig. S2 – *(A) UCRB annual precipitation from PRISM climate normals (1980-2010). (B)-(E) Seasonal precipitation as a percent of annual precipitation in the UCRB for winter, spring, summer, and fall, respectively.*

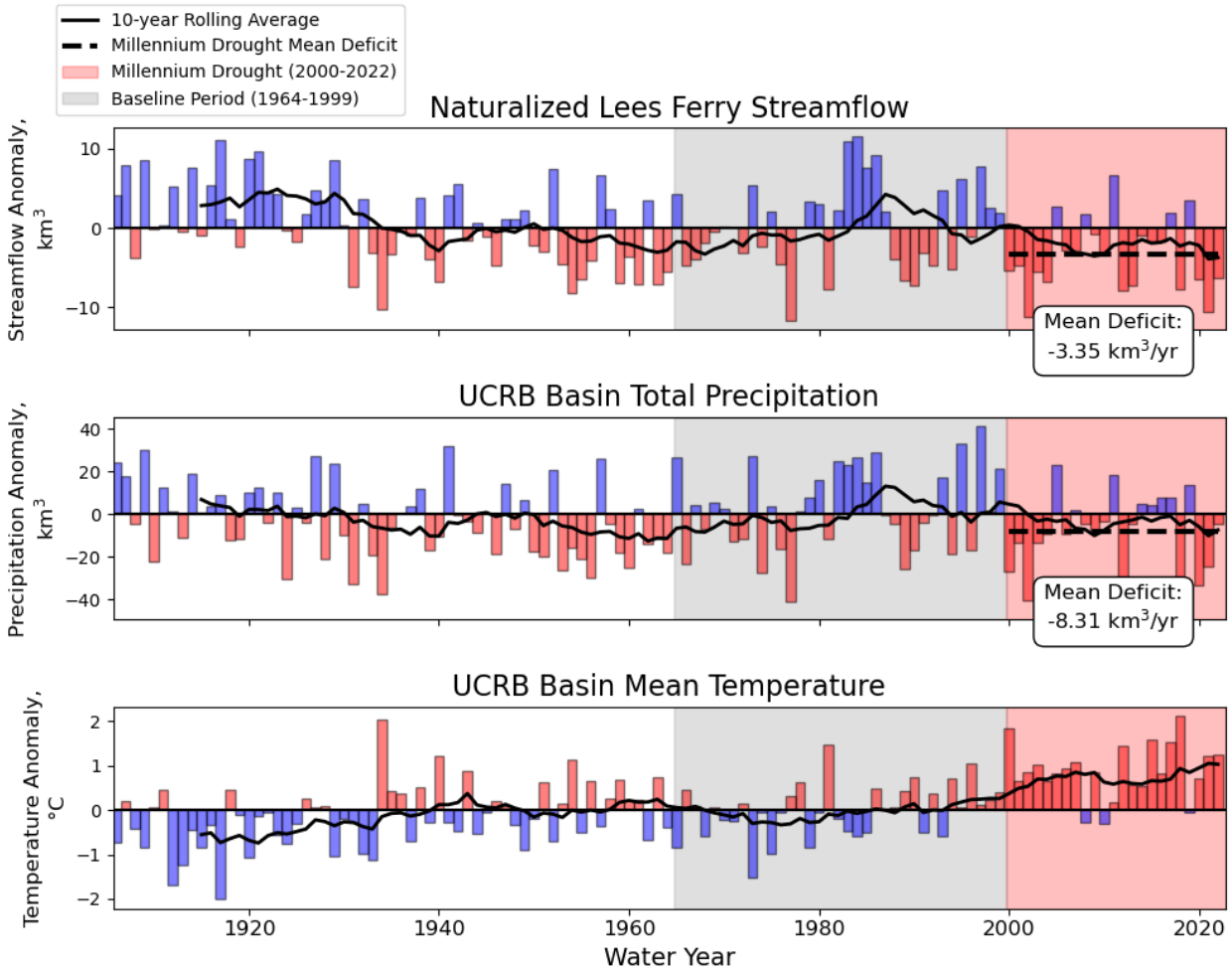

Fig. S3 – *Annual anomalies relative to the baseline average, with 10-year rolling average (black line) for (A) streamflow acquired from the USBR, (B) precipitation acquired from PRISM, and (C) temperature acquired from PRISM over the period of record (1906 to 2022). The mean deficit values, in km³/year during the Millennium Drought are shown in (A) and (B).*

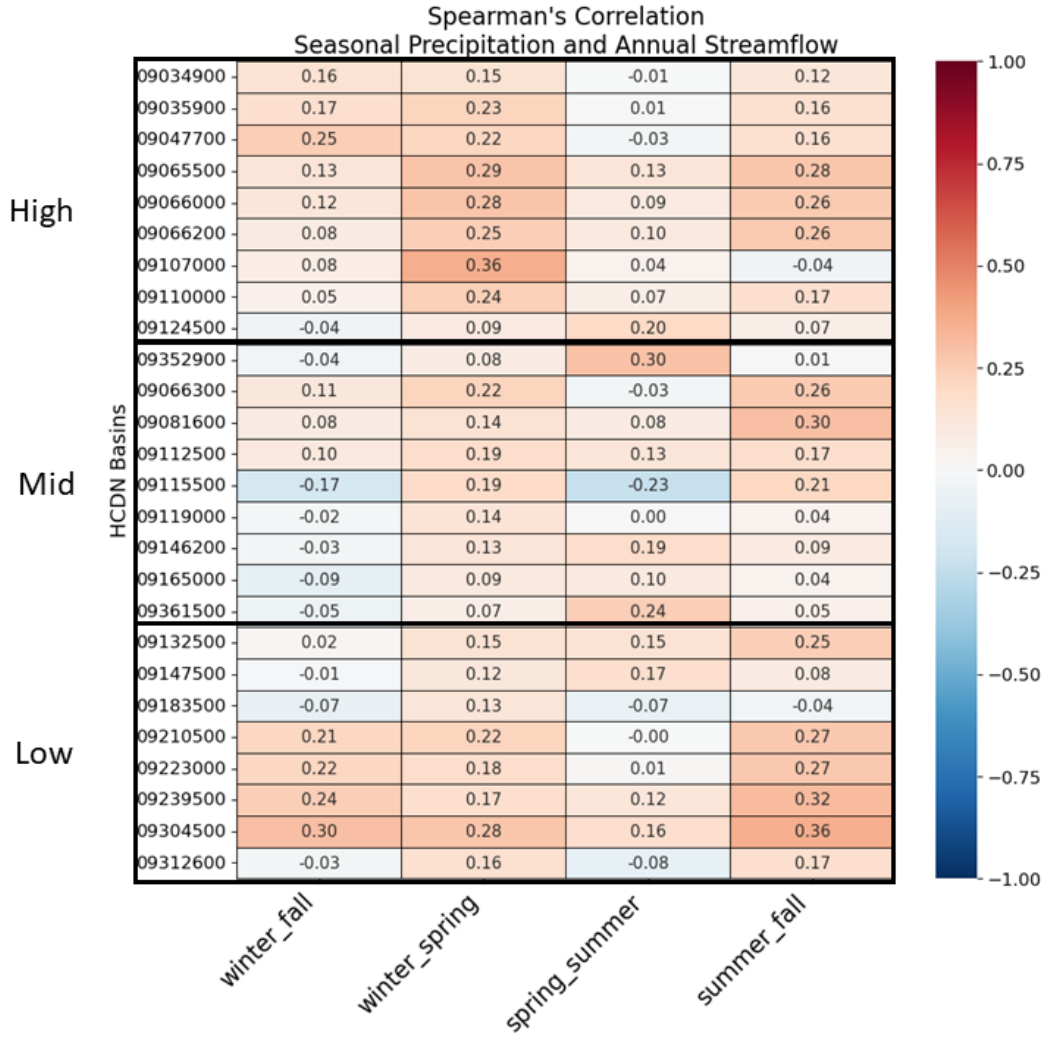

Fig. S4 – *Spearman's rank correlation between seasonal precipitation for each HCDN basin, grouped by low, mid, and high elevations, over the period of analysis. Values range from -1 to 1, with values above +0.5 (or below -0.5) indicating a strong positive (negative) correlation between variables. Note that all values are between -0.23 and +0.36, demonstrating weak correlations in precipitation between adjacent seasons.*

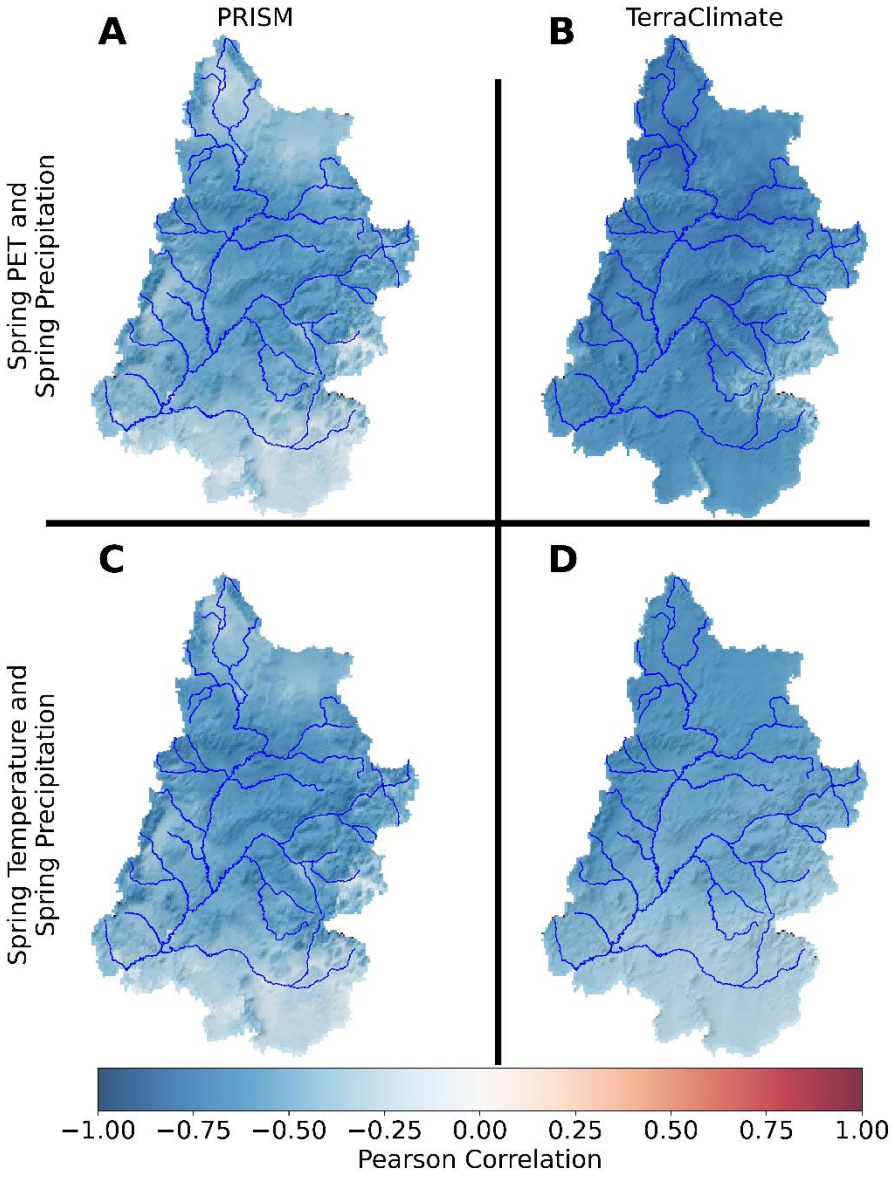

Fig. S5 – *Pearson correlation values between spring precipitation and spring PET estimates (A, B) and spring precipitation and spring temperature (C, D) from PRISM (A, C) and Terraclimate (B, D). Results are colored by correlation values.*

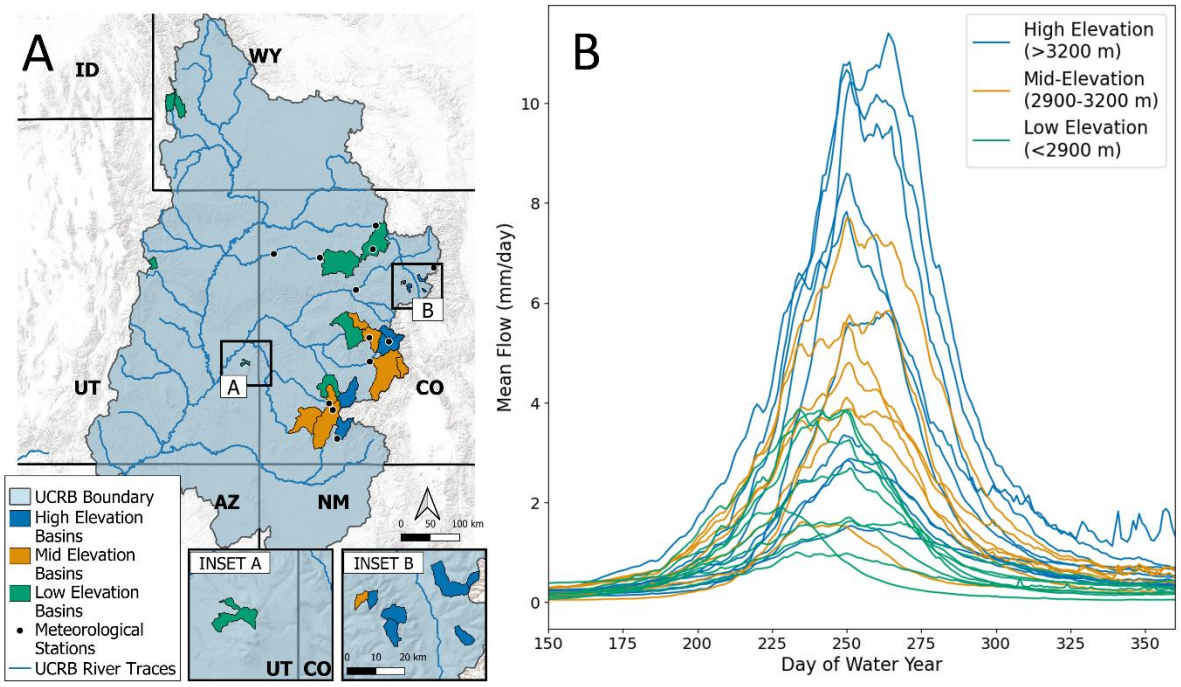

Fig. S6 – *(A) Map of UCRB boundary with high-, mid-, and low-elevation HCDN basin groupings. (B) Average annual hydrograph for each HCDN basin separated by elevation groupings.*

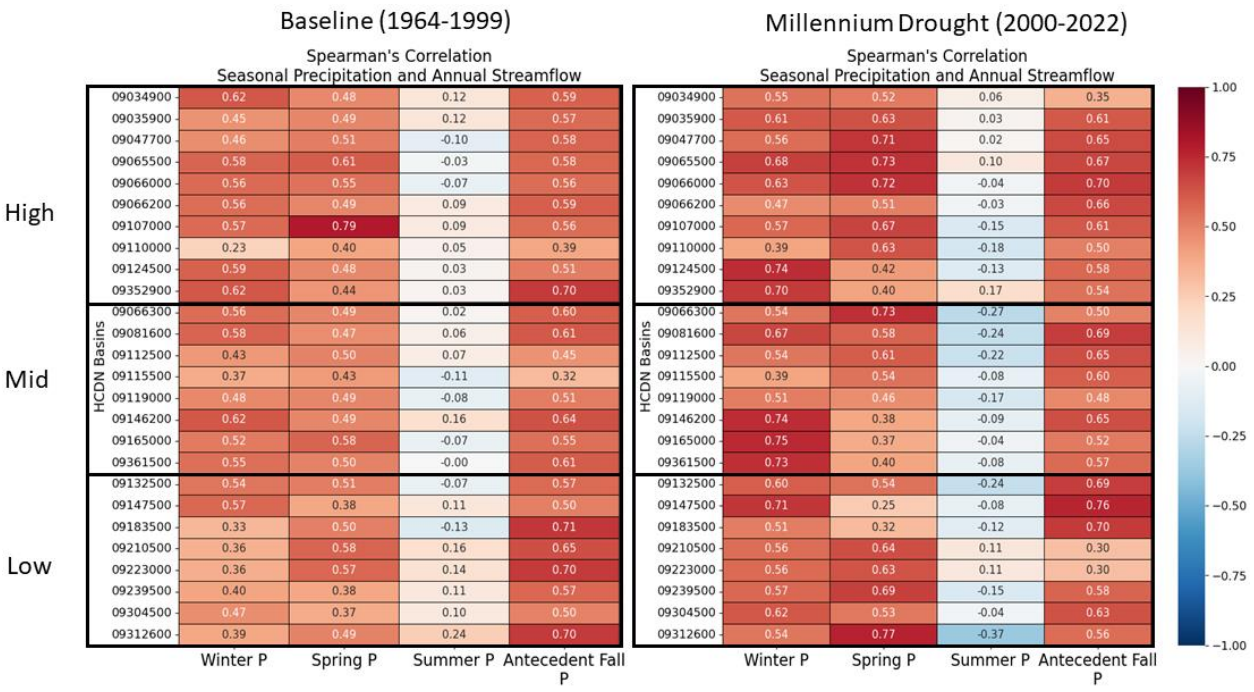

Fig. S7 – *Spearman's rank correlation between seasonal precipitation and annual streamflow for each HCDN basin over the period of analysis. Values range between -1 and 1, with values above +0.5 (or below -0.5) indicating strong positive (negative) correlation between variables.*

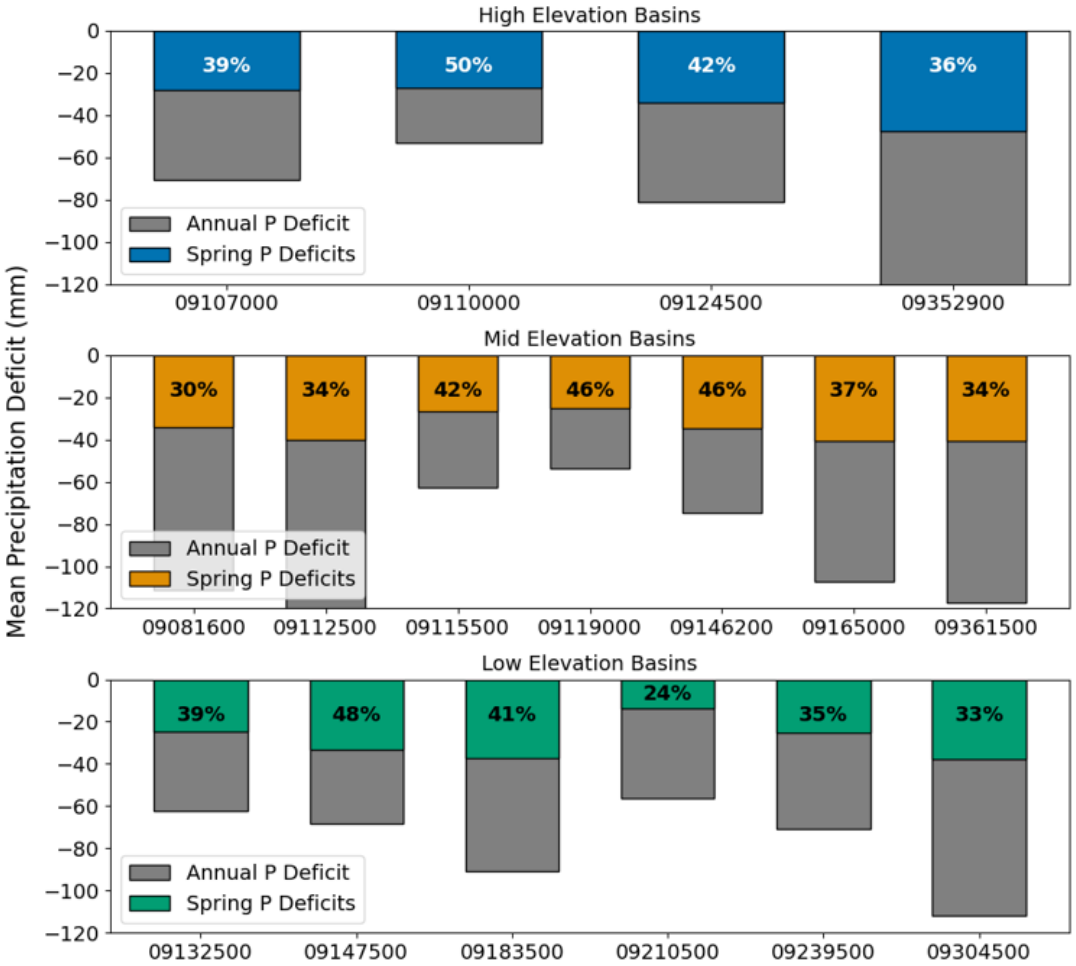

Fig. S8 – *High, mid-, and low- elevation basins with significant annual precipitation deficits between the baseline and Millennium Drought periods (gray) and the percent of the annual deficit accounted for by spring precipitation change (colored).*

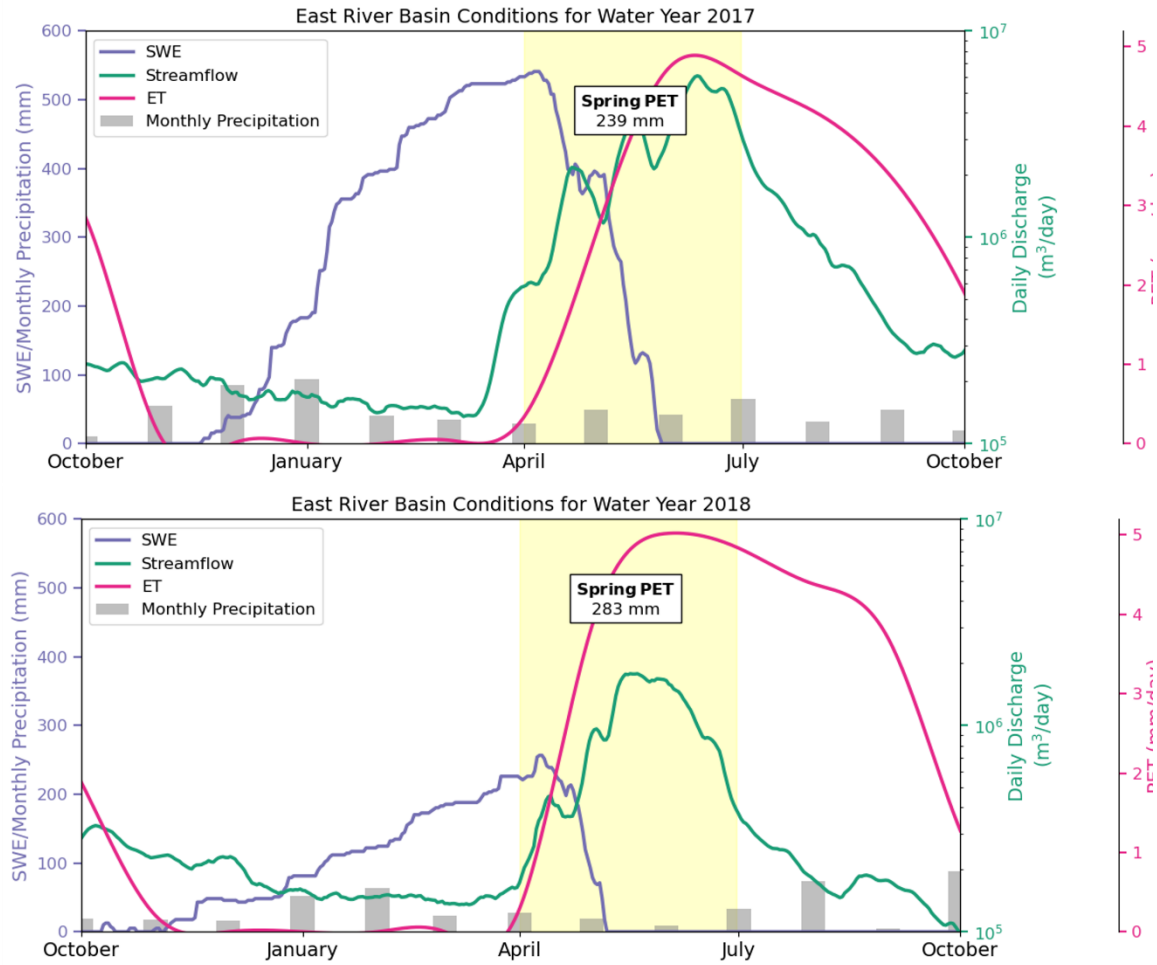

Fig. S9 – *Daily SWE, streamflow, and PET and monthly precipitation over the East River basin for water years 2017 (A) and 2018 (B) which showed dramatically different behavior in response to significant differences in monthly precipitation, particularly in fall and spring. Water year 2018 represents behavior expected from a lower-elevation basin (earlier snowmelt, earlier streamflow timing), wheras water year 2017 represents behavior from a higher-elevation basin, providing a "time-for-space" substitution. The spring period (April through June) is highlighted in yellow, and the total spring PET is shown in the text box. Daily SWE values were acquired from the NRCS Butte SNOTEL site (site ID 380) contained within the East River basin, daily streamflow was acquired from the basin outlet USGS stream gage (ID 9112500), and daily PET and monthly precipitation were estimated from the 1-km WRF model run from Rudisill et al. (2022).*

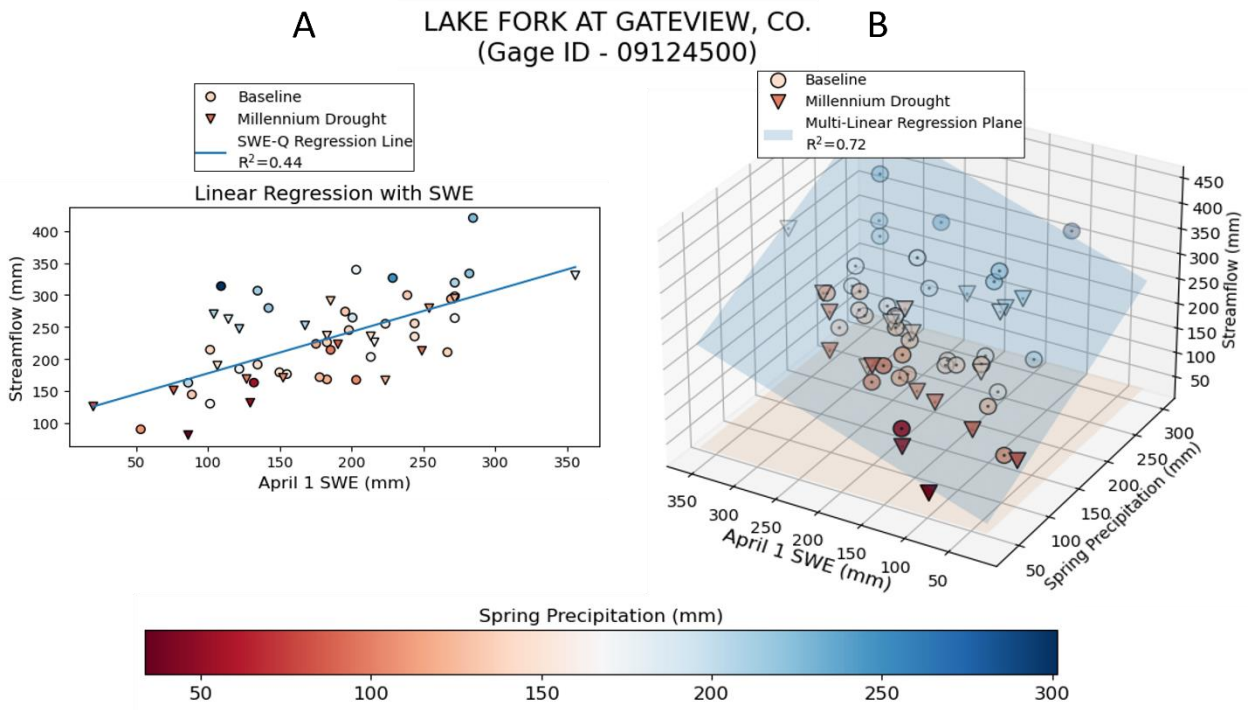

Fig. S10 – *(A) Linear regression results with April 1 SWE estimates from the Lake City snow course (site 07M08) as the independent variable and annual streamflow for the Lake Fork basin as the dependent variable. (B) Multi-linear regression results between SWE and spring precipitation as independent variables and annual streamflow as the dependent variable. Spring precipitation totals color the baseline (circles) and the Millennium Drought (triangles).*

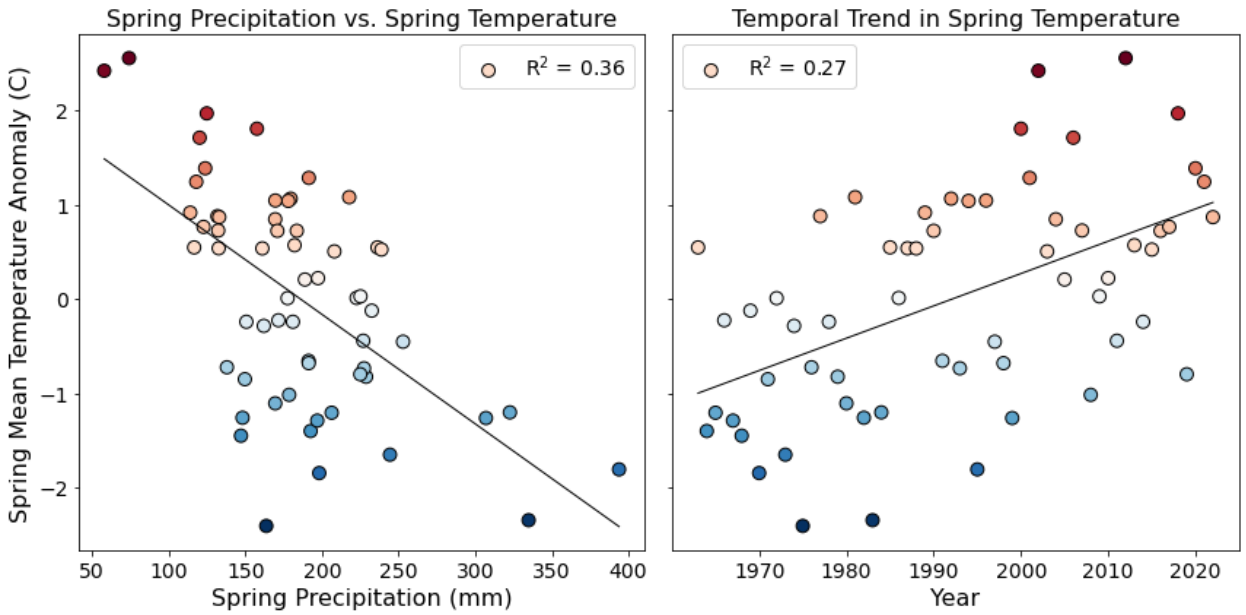

Fig. S11 – *(A) Scatter plot and a best-fit line showing the relationship between spring precipitation and spring temperature anomaly over the UCRB. (B) Temporal trend in spring temperature between 1963 and 2022. Note the greater variance explained in (A) relative to (B). Points in both plots are colored by temperature.*

Supplementary Tables

Table S1 – *26 headwater HCDN basins of the UCRB included in the analysis along with general basin characteristics.*

USGS Gage ID	Site Name	Area-Normalized Basin Mean Elevation (m)	Center-of-Mass (day of year)	Elevation Group	Drainage Area (km^2)	Precipitation (mm)
9034900	BOBTAIL CREEK	3571	169	High	14	744
9035900	SOUTH FORK OF WILLIAMS FORK	3356	163	High	73	692
9047700	KEYSTONE GULCH	3318	152	High	24	498
9065500	GORE CREEK AT UPPER STATION	3380	162	High	38	758
9066000	BLACK GORE CREEK	3257	155	High	32	761
9066200	BOOTH CREEK	3290	159	High	16	694
9107000	TAYLOR RIVER AT TAYLOR PARK	3324	152	High	330	650
9110000	TAYLOR RIVER	3241	160	High	1237	650
9124500	LAKE FORK	3316	160	High	879	733
9352900	VALLECITO CREEK	3223	153	High	188	911
9066300	MIDDLE CREEK	3173	163	Mid	16	567
9081600	CRYSTAL RIVER AB AVALANCHE C	3098	159	Mid	433	963
9112500	EAST RIVER	3127	154	Mid	749	871
9115500	TOMICHI CREEK AT SARGENTS	3102	140	Mid	385	596
9119000	TOMICHI CREEK	2962	134	Mid	2743	485
9146200	UNCOMPAHGRE RIVER	3049	158	Mid	384	729
9165000	DOLORES RIVER	2956	148	Mid	274	795
9361500	ANIMAS RIVER	3036	150	Mid	1838	868
9132500	NORTH FORK GUNNISON RIVER	2708	142	Low	1363	722
9147500	UNCOMPAHGRE RIVER AT COLONA	2816	155	Low	1160	656
9183500	MILL CREEK	2555	130	Low	68	652
9210500	FONTENELLE CREEK	2471	138	Low	400	558
9223000	HAMS FORK	2584	144	Low	328	679
9239500	YAMPA RIVER	2675	145	Low	1460	791
9304500	WHITE RIVER	2737	140	Low	1941	762
9312600	WHITE RIVER BL TABBYUNE	2512	125	Low	196	531

Table S2 - *Annual and seasonal (winter, spring, summer, fall) precipitation changes between the baseline (1964-1999) and the Millennium Drought (2000-2022) for each HCDN basin and the entire UCRB, from PRISM. Each cell shows the difference between period means and the percent difference compared to the baseline period. Student t-test results with p<0.05 are highlighted in red, bolded, and italicized. Student t-test results with 0.05≤p<0.10 are highlighted in yellow and italicized.*

HCDN Basin		Annual Precipitation Change		Winter Precipitation Change		Spring Precipitation Change		Summer Precipitation Change		Fall Precipitation Change	
		Difference (mm) (p-value)	Percent Difference	Difference (mm) (p-value)	Percent Difference	Difference (mm) (p-value)	Percent Difference	Difference (mm) (p-value)	Percent Difference	Difference (mm) (p-value)	Percent Difference
High Elevation Basins	9034900	-7 (0.41)	-1%	+8 (0.70)	4%	-27 (0.17)	-12%	-1 (0.48)	-1%	+5 (0.75)	4%
	9035900	-1 (0.49)	0%	+10 (0.80)	6%	-23 (0.18)	-11%	-1 (0.46)	-1%	+7 (0.75)	4%
	9047700	+19 (0.81)	4%	+16 (0.96)	15%	-6 (0.56)	-5%	+4 (0.64)	3%	+2 (0.72)	2%
	9065500	-8 (0.41)	-1%	+1 (0.51)	0%	-14 (0.48)	-7%	+1 (0.52)	0%	-2 (0.46)	-1%
	9066000	-9 (0.40)	-1%	+3 (0.59)	2%	-18 (0.4)	-9%	+4 (0.60)	2%	-4 (0.35)	-2%
	9066200	+13 (0.66)	2%	+5 (0.66)	3%	-2 (0.51)	-1%	+1 (0.52)	0%	+3 (0.64)	2%
	9107000	***-71 (0.01)***	***-9%***	*-27 (0.06)*	*-12%*	*-28 (0.06)*	*-16%*	-1 (0.46)	-1%	-19 (0.12)	-9%
	9110000	***-53 (0.03)***	***-8%***	*-20 (0.06)*	*-10%*	***-27 (0.02)***	***-17%***	+2 (0.57)	1%	-12 (0.27)	-7%
	9124500	***-81 (0.01)***	***-11%***	-10 (0.27)	-5%	***-34 (0.005)***	***-21%***	-12 (0.22)	-6%	*-28 (0.06)*	*-13%*
	9352900	***-121 (0.003)***	***-13%***	-20 (0.24)	-8%	***-48 (0.001)***	***-26%***	*-34 (0.05)*	*-13%*	-34 (0.10)	-13%
Mid-Elevation Basins	9066300	+23 (0.83)	4%	+11 (0.85)	7%	0 (0.73)	0%	+6 (0.73)	5%	+1 (0.58)	1%
	9081600	***-111 (0.01)***	***11%***	***-53 (0.01)***	***-16%***	***-34 (0.04)***	***-16%***	+9 (0.72)	5%	*-36 (0.06)*	*-12%*
	9112500	***-120 (0.001)***	***13%***	***-48 (0.01)***	***-16%***	***-40 (0.01)***	***-20%***	+3 (0.60)	2%	***-40 (0.03)***	***-15%***
	9115500	***-63 (0.01)***	***10%***	-17 (0.14)	-10%	***-27 (0.01)***	***-18%***	-10 (0.21)	-6%	-13 (0.20)	-9%
	9119000	***-54 (0.002)***	***11%***	-8 (0.22)	-7%	***-25 (0.003)***	***-21%***	-10 (0.17)	-7%	*-12 (0.09)*	*-10%*
	9146200	***-75 (0.01)***	***10%***	-6 (0.37)	-3%	***-35 (0.01)***	***-21%***	-10 (0.26)	-5%	***-27 (0.04)***	***-13%***
	9165000	***-107 (0.02)***	***13%***	-22 (0.18)	-9%	***-41 (0.002)***	***-25%***	-20 (0.12)	-9%	*-29 (0.08)*	*-13%*
	9361500	***-117 (0.03)***	***13%***	-22 (0.21)	-8%	***-41 (0.004)***	***-24%***	*-25 (0.08)*	*-11%*	*-37 (0.06)*	*-14%*
Low-Elevation Basins	9132500	***-62 (0.03)***	***-8%***	*-24 (0.09)*	*-11%*	***-25 (0.05)***	***-15%***	+6 (0.67)	4%	-21 (0.10)	-10%
	9147500	***-68 (0.01)***	***-10%***	-6 (0.34)	-3%	***-33 (0.01)***	***-22%***	-8 (0.28)	-44%	*-23 (0.05)*	*-13%*
	9183500	***-91 (0.01)***	***-13%***	*-29 (0.08)*	*-15%*	***-37 (0.01)***	***-26%***	-3 (0.44)	-2%	-23 (0.13)	-12%
	9210500	***-56 (0.04)***	***-9%***	-15 (0.18)	-8%	-14 (0.146)	-9%	*-14 (0.09)*	*-16%*	-15 (0.15)	-9%
	9223000	*-63 (0.06)*	*-8%*	-20 (0.17)	-8%	-11 (0.229)	-6%	-14 (0.11)	-14%	-20 (0.14)	-9%
	9239500	***-71 (0.02)***	***-9%***	*-27 (0.05)*	*-10%*	*-25 (0.06)*	*-12%*	-6 (0.32)	-4%	*-19 (0.09)*	*-8%*
	9304500	***-112 (0.01)***	***-14%***	***-44 (0.01)***	***-18%***	***-38 (0.01)***	***-19%***	-1 (0.58)	-1%	***-34 (0.01)***	***-15%***
	9312600	-35 (0.12)	-6%	-15 (0.16)	-8%	***-19 (0.04)***	***-15%***	-1 (0.46)	-1%	-3 (0.43)	-2%
UCRB		***-28 (0.04)***	***-7%***	-6 (0.19)	-6%	***-16 (0.01)***	***-17%***	-6 (0.32)	-5%	-9 (0.14)	-9%

Table S3 – *Basin-normalized volume change in millimeters depth and center of mass timing change in days between the baseline and Millennium Drought periods. Each cell shows the difference between period means along with the percent difference compared to the baseline period for the volume change. Student t-test results with p<0.05 are highlighted in red, bolded, and italicized. Student t-test results with 0.05≤p<0.10 are highlighted in yellow and italicized.*

HCDN Basin		Volume Change	
		Difference (mm) (p-value)	Percent Difference
High Elevation Basins	9034900	*-71 (0.09)*	*-10%*
	9035900	-9 (0.51)	-2%
	9047700	-25 (0.26)	-10%
	9065500	*-81 (0.08)*	*-11%*
	9066000	-46 (0.13)	-10%
	9066200	*-91 (0.06)*	*-14%*
	9107000	*-48 (0.08)*	*-15%*
	9110000	***-46 (0.004)***	***-19%***
	9124500	*-25 (0.09)*	*-11%*
	9352900	***-112 (0.03)***	***-16%***
Mid-Elevation Basins	9066300	**-62 (0.04)**	**-18%**
	9081600	***-81 (0.04)***	**-13%**
	9112500	***-66 (0.02)***	**-16%**
	9115500	*-18 (0.09)*	*-12%*
	9119000	***-13 (0.01)***	**-23%**
	9146200	***-47 (0.04)***	**-12%**
	9165000	***-93 (0.01)***	**-21%**
	9361500	***-79 (0.01)***	**-20%**
Low-Elevation Basins	9132500	***-72 (0.02)***	***-22%***
	9147500	***-40 (0.03)***	***-19%***
	9183500	***-47 (0.003)***	***-29%***
	9210500	*-23 (0.08)*	*-14%*
	9223000	***-70 (0.01)***	***-25%***
	9239500	*-31 (0.08)*	*-11%*
	9304500	***-44 (0.01)***	***-15%***
	9312600	***-54 (0.001)***	***-41%***
UCRB		***-12 (0.01)***	***-19%***

Table S4 *Precipitation gage station ID, name, location, and elevation for the 11 gages used to validate the results from PRISM.*

STATION	NAME	LATITUDE	LONGITUDE	ELEVATION (m)
USC00051959	CRESTED BUTTE, CO US	38.8738	-106.9772	2702.7
USC00053662	GUNNISON 3 SW, CO US	38.5254	-106.9672	2323.2
USC00056832	RANGELY 1 E, CO US	40.0889	-108.7727	1608.4
USC00057618	SHOSHONE, CO US	39.5703	-107.2267	1826.4
USC00057656	SILVERTON, CO US	37.8088	-107.6633	2830.1
USC00057936	STEAMBOAT SPRINGS, CO US	40.4883	-106.8233	2092.8
USC00058064	SUGARLOAF RESERVOIR, CO U	39.2495	-106.3713	2968.1
USC00058184	TAYLOR PARK, CO US	38.8183	-106.6086	2797.8
USC00058204	TELLURIDE 4 WNW, CO US	37.9493	-107.8736	2635.3
USC00058501	TWIN LAKES RESERVOIR, CO U	39.09419	-106.35064	2815.1
USC00058582	VALLECITO DAM, CO US	37.3805	-107.5812	2329.9
USC00059175	WINTER PARK, CO US	39.8898	-105.76206	2772.2
USC00059265	YAMPA, CO US	40.15628	-106.91085	2394.8

Table S5 – *Datasets and URL access for the data*

Dataset	URL and data accessed
PRISM 4-km monthly precipitation and temperature (1964-2022)	https://prism.oregonstate.edu/ Accessed 24 April 2023
UCRB basin boundary	https://www.sciencebase.gov/catalog/item/4f4e4a38e4b07f02db61cebb Accessed 17 April 2023
HCDN Basins derived from GAGES II: Geospatial Attributes of Gages for Evaluating Streamflow	https://water.usgs.gov/GIS/metadata/usgswrd/XML/gagesII_Sept2011.xml Accessed 17 April 2023
National Center for Environmental Information Climate Data Online service	https://www.ncdc.noaa.gov/cdo-web/ Accessed 25 July 2023
USGS daily stream gage data from the National Water Information System (NWIS)	https://waterdata.usgs.gov/nwis Accessed 26 April 2023
3DEP from USGS National Map	https://www.usgs.gov/programs/national-geospatial-program/national-map Accessed 6 July 2023
USBR Naturalized Streamflow	https://www.usbr.gov/lc/region/g4000/NaturalFlow/provisional.html Accessed 24 April 2023
Fractional tree-covered area from the National Land Cover Dataset	https://www.mrlc.gov/data Accessed 6 July 2023
Snowmelt Timing Maps Derived from MODIS for North America	https://daac.ornl.gov/cgi-bin/dsviewer.pl?ds_id=1712 Accessed 17 October 2023
NRCS Snow Course Data	https://www.nrcs.usda.gov/resources/data-and-reports/snow-and-climate-monitoring-predefined-reports-and-maps Accessed 4 August 2023
Monthly TerraClimate Data (1964-2022)	https://www.climatologylab.org/terraclimate.html. Accessed 18 August 2023

References

Abatzoglou, J. T., Dobrowski, S. Z., Parks, S. A., & Hegewisch, K. C. (2018). TerraClimate, a high-resolution global dataset of monthly climate and climatic water balance from 1958–2015. *Scientific Data*, *5*(1), Article 1. https://doi.org/10.1038/sdata.2017.191

Barnhart, T. B., Molotch, N. P., Livneh, B., Harpold, A. A., Knowles, J. F., & Schneider, D. (2016). Snowmelt rate dictates streamflow. *Geophysical Research Letters*, *43*(15), 8006–8016. https://doi.org/10.1002/2016GL069690

Bass, B., Goldenson, N., Rahimi, S., & Hall, A. (2023). Aridification of Colorado River Basin's Snowpack Regions Has Driven Water Losses Despite Ameliorating Effects of Vegetation. *Water Resources Research*, *59*(7), e2022WR033454. https://doi.org/10.1029/2022WR033454

Bennett, A., Nijssen, B., Ou, G., Clark, M., & Nearing, G. (2019). Quantifying Process Connectivity With Transfer Entropy in Hydrologic Models. *Water Resources Research*, *55*(6), 4613–4629. https://doi.org/10.1029/2018WR024555

Betts, A. K., Desjardins, R., Worth, D., & Beckage, B. (2014). Climate coupling between temperature, humidity, precipitation, and cloud cover over the Canadian Prairies. *Journal of Geophysical Research: Atmospheres*, *119*(23), 13,305-13,326. https://doi.org/10.1002/2014JD022511

Biederman, J. A., Robles, M. D., Scott, R. L., & Knowles, J. F. (2022). Streamflow Response to Wildfire Differs With Season and Elevation in Adjacent Headwaters of the Lower Colorado River Basin. *Water Resources Research*, *58*(3), e2021WR030687. https://doi.org/10.1029/2021WR030687

Bohr, G. S., & Aguado, E. (2001). Use of April 1 SWE measurements as estimates of peak seasonal snowpack and total cold-season precipitation. *Water Resources Research*, *37*(1), 51–60. https://doi.org/10.1029/2000WR900256

Brooks, P. D., Gelderloos, A., Wolf, M. A., Jamison, L. R., Strong, C., Solomon, D. K., Bowen, G. J., Burian, S., Tai, X., Arens, S., Briefer, L., Kirkham, T., & Stewart, J. (2021). Groundwater-Mediated Memory of Past Climate Controls Water Yield in Snowmelt-Dominated Catchments. *Water Resources Research*, *57*(10), e2021WR030605. https://doi.org/10.1029/2021WR030605

Carroll, R. W. H., Bearup, L. A., Brown, W., Dong, W., Bill, M., & Willlams, K. H. (2018). Factors controlling seasonal groundwater and solute flux from snow-dominated basins. *Hydrological Processes*, *32*(14), 2187–2202. https://doi.org/10.1002/hyp.13151

Carroll, R. W. H., Deems, J. S., Niswonger, R., Schumer, R., & Williams, K. H. (2019). The Importance of Interflow to Groundwater Recharge in a Snowmelt-Dominated Headwater Basin. *Geophysical Research Letters*, *46*(11), 5899–5908. https://doi.org/10.1029/2019GL082447

Carroll, R. W. H., Gochis, D., & Williams, K. H. (2020). Efficiency of the Summer Monsoon in Generating Streamflow Within a Snow-Dominated Headwater Basin of the Colorado River. *Geophysical Research Letters*, *47*(23), e2020GL090856. https://doi.org/10.1029/2020GL090856

Castle, S. L., Thomas, B. F., Reager, J. T., Rodell, M., Swenson, S. C., & Famiglietti, J. S. (2014). Groundwater depletion during drought threatens future water security of the Colorado River Basin. *Geophysical Research Letters*, *41*(16), 5904–5911. https://doi.org/10.1002/2014GL061055

Cayan, D. R., Kammerdiener, S. A., Dettinger, M. D., Caprio, J. M., & Peterson, D. H. (2001). Changes in the Onset of Spring in the Western United States. *Bulletin of the American Meteorological Society*, *82*(3), 399–416. https://doi.org/10.1175/1520-0477(2001)082<0399:CITOOS>2.3.CO;2

Christensen, N. S., & Lettenmaier, D. P. (2007). A multimodel ensemble approach to assessment of climate change impacts on the hydrology and water resources of the

Colorado River Basin. *Hydrology and Earth System Sciences*, *11*(4), 1417–1434. https://doi.org/10.5194/hess-11-1417-2007

Christensen, N. S., Wood, A. W., Voisin, N., Lettenmaier, D. P., & Palmer, R. N. (2004). The Effects of Climate Change on the Hydrology and Water Resources of the Colorado River Basin. *Climatic Change*, *62*(1), 337–363. https://doi.org/10.1023/B:CLIM.0000013684.13621.1f

Clow, D. W. (2010). Changes in the Timing of Snowmelt and Streamflow in Colorado: A Response to Recent Warming. *Journal of Climate*, *23*(9), 2293–2306. https://doi.org/10.1175/2009JCLI2951.1

Daly, C., Halbleib, M., Smith, J. I., Gibson, W. P., Doggett, M. K., Taylor, G. H., Curtis, J., & Pasteris, P. P. (2008). Physiographically sensitive mapping of climatological temperature and precipitation across the conterminous United States. *International Journal of Climatology*, *28*(15), 2031–2064. https://doi.org/10.1002/joc.1688

Fassnacht, S. R., Dressler, K. A., & Bales, R. C. (2003). Snow water equivalent interpolation for the Colorado River Basin from snow telemetry (SNOTEL) data. *Water Resources Research*, *39*(8). https://doi.org/10.1029/2002WR001512

Fatichi, S., Ivanov, V. Y., & Caporali, E. (2012). Investigating Interannual Variability of Precipitation at the Global Scale: Is There a Connection with Seasonality? *Journal of Climate*, *25*(16), 5512–5523. https://doi.org/10.1175/JCLI-D-11-00356.1

Ficklin, D. L., Stewart, I. T., & Maurer, E. P. (2013). Climate Change Impacts on Streamflow and Subbasin-Scale Hydrology in the Upper Colorado River Basin. *PLOS ONE*, *8*(8), e71297. https://doi.org/10.1371/journal.pone.0071297

Fleck, J., & Udall, B. (2021). Managing Colorado River risk. *Science (New York, N.Y.)*, *372*(6545), 885. https://doi.org/10.1126/science.abj5498

Foster, L. M., Bearup, L. A., Molotch, N. P., Brooks, P. D., & Maxwell, R. M. (2016). Energy budget increases reduce mean streamflow more than snow–rain transitions: Using integrated modeling to isolate climate change impacts on Rocky Mountain hydrology. *Environmental Research Letters*, *11*(4), 044015. https://doi.org/10.1088/1748-9326/11/4/044015

Fritze, H., Stewart, I. T., & Pebesma, E. (2011). Shifts in Western North American Snowmelt Runoff Regimes for the Recent Warm Decades. *Journal of Hydrometeorology*, *12*(5), 989–1006. https://doi.org/10.1175/2011JHM1360.1

Gangopadhyay, S., Woodhouse, C. A., McCabe, G. J., Routson, C. C., & Meko, D. M. (2022). Tree Rings Reveal Unmatched 2nd Century Drought in the Colorado River Basin. *Geophysical Research Letters*, *49*(11), e2022GL098781. https://doi.org/10.1029/2022GL098781

Gordon, B. L., Brooks, P. D., Krogh, S. A., Boisrame, G. F. S., Carroll, R. W. H., McNamara, J. P., & Harpold, A. A. (2022). Why does snowmelt-driven streamflow response to warming vary? A data-driven review and predictive framework. *Environmental Research Letters*, *17*(5), 053004. https://doi.org/10.1088/1748-9326/ac64b4

Gray, S. T., Lukas, J. J., & Woodhouse, C. A. (2011). Millennial-Length Records of Streamflow From Three Major Upper Colorado River Tributaries1. *JAWRA Journal of the American Water Resources Association*, *47*(4), 702–712. https://doi.org/10.1111/j.1752-1688.2011.00535.x

Guentchev, G., Barsugli, J. J., & Eischeid, J. (2010). Homogeneity of Gridded Precipitation Datasets for the Colorado River Basin. *Journal of Applied Meteorology and Climatology*, *49*(12), 2404–2415. https://doi.org/10.1175/2010JAMC2484.1

Harpold, A. A., Sutcliffe, K., Clayton, J., Goodbody, A., & Vazquez, S. (2017). Does Including Soil Moisture Observations Improve Operational Streamflow Forecasts in Snow-Dominated Watersheds? *JAWRA Journal of the American Water Resources Association*, *53*(1), 179–196. https://doi.org/10.1111/1752-1688.12490

Heldmyer, A. J., Bjarke, N. R., & Livneh, B. (2022). A 21st-Century perspective on snow drought in the Upper Colorado River Basin. *JAWRA Journal of the American Water Resources Association*, *n/a*(n/a). https://doi.org/10.1111/1752-1688.13095

Henn, B., Newman, A. J., Livneh, B., Daly, C., & Lundquist, J. D. (2018). An assessment of differences in gridded precipitation datasets in complex terrain. *Journal of Hydrology*, *556*, 1205–1219. https://doi.org/10.1016/j.jhydrol.2017.03.008

Hoerling, M., Barsugli, J., Livneh, B., Eischeid, J., Quan, X., & Badger, A. (2019). Causes for the Century-Long Decline in Colorado River Flow. *Journal of Climate*, *32*(23), 8181–8203. https://doi.org/10.1175/JCLI-D-19-0207.1

Hutchison, B. A. (1966). A Comparison of Evaporation from Snow and Soil Surfaces. *International Association of Scientific Hydrology. Bulletin*, *11*(1), 34–42. https://doi.org/10.1080/02626666609493439

Kalra, A., & Ahmad, S. (2011). Evaluating changes and estimating seasonal precipitation for the Colorado River Basin using a stochastic nonparametric disaggregation technique. *Water Resources Research*, *47*(5). https://doi.org/10.1029/2010WR009118

Knowles, N., & Cayan, D. R. (2004). Elevational Dependence of Projected Hydrologic Changes in the San Francisco Estuary and Watershed. *Climatic Change*, *62*(1), 319–336. https://doi.org/10.1023/B:CLIM.0000013696.14308.b9

Lapides, D. A., Hahm, W. J., Rempe, D. M., Whiting, J., & Dralle, D. N. (2022). Causes of Missing Snowmelt Following Drought. *Geophysical Research Letters*, *49*(19), e2022GL100505. https://doi.org/10.1029/2022GL100505

Lehner, F., Wood, A. W., Llewellyn, D., Blatchford, D. B., Goodbody, A. G., & Pappenberger, F. (2017). Mitigating the Impacts of Climate Nonstationarity on Seasonal Streamflow Predictability in the U.S. Southwest. *Geophysical Research Letters*, *44*(24), 12,208-12,217. https://doi.org/10.1002/2017GL076043

Li, D., Wrzesien, M. L., Durand, M., Adam, J., & Lettenmaier, D. P. (2017). How much runoff originates as snow in the western United States, and how will that change in the future? *Geophysical Research Letters*, *44*(12), 6163–6172. https://doi.org/10.1002/2017GL073551

Lukas, J., & Payton, E. (2020). *Colorado River Basin Climate and Hydrology: State of the Science*. https://doi.org/10.25810/3HCV-W477

Lundquist, J. D., Cayan, D. R., & Dettinger, M. D. (2004). Spring Onset in the Sierra Nevada: When Is Snowmelt Independent of Elevation? *Journal of Hydrometeorology*, *5*(2), 327–342. https://doi.org/10.1175/1525-7541(2004)005<0327:SOITSN>2.0.CO;2

Lundquist, J. D., Hughes, M., Henn, B., Gutmann, E. D., Livneh, B., Dozier, J., & Neiman, P. (2015). High-Elevation Precipitation Patterns: Using Snow Measurements to Assess Daily Gridded Datasets across the Sierra Nevada, California. *Journal of Hydrometeorology*, *16*(4), 1773–1792. https://doi.org/10.1175/JHM-D-15-0019.1

Mahanama, S., Livneh, B., Koster, R., Lettenmaier, D., & Reichle, R. (2012). Soil Moisture, Snow, and Seasonal Streamflow Forecasts in the United States. *Journal of Hydrometeorology*, *13*(1), 189–203. https://doi.org/10.1175/JHM-D-11-046.1

Massari, C., Avanzi, F., Bruno, G., Gabellani, S., Penna, D., & Camici, S. (2022). Evaporation enhancement drives the European water-budget deficit during multi-year droughts. *Hydrology and Earth System Sciences*, *26*(6), 1527–1543. https://doi.org/10.5194/hess-26-1527-2022

Mayer, T. D., & Naman, S. W. (2011). Streamflow Response to Climate as Influenced by Geology and Elevation1. *JAWRA Journal of the American Water Resources Association*, *47*(4), 724–738. https://doi.org/10.1111/j.1752-1688.2011.00537.x

McAfee, S. A., & Russell, J. L. (2008). Northern Annular Mode impact on spring climate in the western United States. *Geophysical Research Letters*, *35*(17). https://doi.org/10.1029/2008GL034828

McCabe, G. J., & Clark, M. P. (2005). Trends and Variability in Snowmelt Runoff in the Western United States. *Journal of Hydrometeorology*, *6*(4), 476–482. https://doi.org/10.1175/JHM428.1

McCabe, G. J., & Wolock, D. M. (2007). Warming may create substantial water supply shortages in the Colorado River basin. *Geophysical Research Letters*, *34*(22). https://doi.org/10.1029/2007GL031764

McCabe, G. J., & Wolock, D. M. (2011). Independent effects of temperature and precipitation on modeled runoff in the conterminous United States. *Water Resources Research*, *47*(11). https://doi.org/10.1029/2011WR010630

McCabe, G. J., Wolock, D. M., Pederson, G. T., Woodhouse, C. A., & McAfee, S. (2017). Evidence that Recent Warming is Reducing Upper Colorado River Flows. *Earth Interactions*, *21*(10), 1–14. https://doi.org/10.1175/EI-D-17-0007.1

McEvoy, D. J., & Hatchett, B. J. (2023). Spring heat waves drive record western United States snow melt in 2021. *Environmental Research Letters*, *18*(1), 014007. https://doi.org/10.1088/1748-9326/aca8bd

Meira Neto, A. A., Niu, G.-Y., Roy, T., Tyler, S., & Troch, P. A. (2020). Interactions between snow cover and evaporation lead to higher sensitivity of streamflow to temperature. *Communications Earth & Environment*, *1*(1), Article 1. https://doi.org/10.1038/s43247-020-00056-9

Miller, M. P. (2012). The influence of reservoirs, climate, land use and hydrologic conditions on loads and chemical quality of dissolved organic carbon in the Colorado River. *Water Resources Research*, *48*(12). https://doi.org/10.1029/2012WR012312

Miller, M. P., Buto, S. G., Susong, D. D., & Rumsey, C. A. (2016). The importance of base flow in sustaining surface water flow in the Upper Colorado River Basin. *Water Resources Research*, *52*(5), 3547–3562. https://doi.org/10.1002/2015WR017963

Miller, R., Schmidt, G. A., & Shindell, D. T. (2006). Forced annular variations in the 20th century Intergovernmental Panel on Climate Change Fourth Assessment Report models. *Journal of Geophysical Research: Atmospheres*, *111*(D18). https://doi.org/10.1029/2005JD006323

Modi, P. A., Small, E. E., Kasprzyk, J., & Livneh, B. (2022). Investigating the Role of Snow Water Equivalent on Streamflow Predictability during Drought. *Journal of Hydrometeorology*, *23*(10), 1607–1625. https://doi.org/10.1175/JHM-D-21-0229.1

Moore, C. (2012). *A climatological study of snow covered areas in the western United States* [M.S., Colorado State University]. https://www.proquest.com/docview/1020419036/abstract/B5141253E392497DPQ/1

Mote, P. W. (2006). Climate-Driven Variability and Trends in Mountain Snowpack in Western North America. *Journal of Climate*, *19*(23), 6209–6220. https://doi.org/10.1175/JCLI3971.1

National Centers for Environmental Information. (n.d.). *Climate Data Online* [dataset]. Retrieved July 21, 2023, from https://www.ncdc.noaa.gov/cdo-web/

Nowak, K., Hoerling, M., Rajagopalan, B., & Zagona, E. (2012). Colorado River Basin Hydroclimatic Variability. *Journal of Climate*, *25*(12), 4389–4403. https://doi.org/10.1175/JCLI-D-11-00406.1

O'Leary, D., Hall, D. K., Medler, M., Matthews, R., & Flower, A. (2020). Snowmelt Timing Maps Derived from MODIS for North America, Version 2, 2001-2018. *ORNL DAAC*. https://doi.org/10.3334/ORNLDAAC/1712

O'Leary, D., Hall, D., Medler, M., & Flower, A. (2018). Quantifying the early snowmelt event of 2015 in the Cascade Mountains, USA by developing and validating MODIS-based snowmelt timing maps. *Frontiers of Earth Science*, *12*(4), 693–710. https://doi.org/10.1007/s11707-018-0719-7

Pagano, T., Wood, A. W., Ramos, M.-H., Cloke, H. L., Pappenberger, F., Clark, M. P., Cranston, M., Kavetski, D., Mathevet, T., Sorooshian, S., & Verkade, J. S. (2014). Challenges of Operational River Forecasting. *Journal of Hydrometeorology*, *15*(4), 1692–1707. https://doi.org/10.1175/JHM-D-13-0188.1

Palmer, P. L. (1988). *The SCS snow survey water supply forecasting program: Current operations and future directions.* Proc. 56th Annual Western Snow Conf., Kalispell, MT.

Pribulick, C. E., Foster, L. M., Bearup, L. A., Navarre-Sitchler, A. K., Williams, K. H., Carroll, R. W. H., & Maxwell, R. M. (2016). Contrasting the hydrologic response due to land cover and climate change in a mountain headwaters system: Contrasting hydrologic response from land cover and climate change. *Ecohydrology*, *9*(8), 1431–1438. https://doi.org/10.1002/eco.1779

PRISM Climate Group, O. S. U. (2014). [dataset]. https://prism.oregonstate.edu

Raleigh, M. S., & Lundquist, J. D. (2012). Comparing and combining SWE estimates from the SNOW-17 model using PRISM and SWE reconstruction. *Water Resources Research*, *48*(1). https://doi.org/10.1029/2011WR010542

Rudisill, W., Vincent, A., Nash, C., & Flores, A. (2022). *Dynamically Downscaled (WRF) 1km, Hourly Meteorological Conditions 1987-2020. East/Taylor Watersheds*. Environmental System Science Data Infrastructure for a Virtual Ecosystem (ESS-DIVE) (United States); Science Area 1: Standard Award: Model-Data Fusion to Examine Multiscale Dynamical Controls on Snow Cover and Critical Zone Moisture Inputs. https://doi.org/10.15485/1845448

Ryken, A. E. C., Gochis, D., & Maxwell, R. (2020). *Unraveling groundwater contributions to evapotranspiration in a mountain headwaters: Using eddy covariance to constrain water and energy fluxes in the East River Watershed* [Preprint]. Preprints. https://doi.org/10.22541/au.159559979.93668749

Salehabadi, H., Tarboton, D. G., Udall, B., Wheeler, K. G., & Schmidt, J. C. (2022). An Assessment of Potential Severe Droughts in the Colorado River Basin. *JAWRA Journal of the American Water Resources Association*, *58*(6), 1053–1075. https://doi.org/10.1111/1752-1688.13061

Schmidt, J. C., Yackulic, C. B., & Kuhn, E. (2023). The Colorado River water crisis: Its origin and the future. *WIREs Water*, *n/a*(n/a), e1672. https://doi.org/10.1002/wat2.1672

Schwartz, M. D., & Reiter, B. E. (2000). Changes in North American spring. *International Journal of Climatology*, *20*(8), 929–932. https://doi.org/10.1002/1097-0088(20000630)20:8<929::AID-JOC557>3.0.CO;2-5

Slack, J. R., Lumb, A. M., & Landwehr, J. M. (1994). *Hydro-Climatic Data Network (HCDN)—A USGS Streamflow Data Set for the U.S. for the Study of Climate Fluctuations* (1.0) [Map]. U.S. Geological Survey. https://water.usgs.gov/GIS/metadata/usgswrd/XML/hcdn.xml

Sprenger, M., Carroll, R. W. H., Dennedy-Frank, J., Siirila-Woodburn, E. R., Newcomer, M. E., Brown, W., Newman, A., Beutler, C., Bill, M., Hubbard, S. S., & Williams, K. H. (2022). Variability of Snow and Rainfall Partitioning Into Evapotranspiration and Summer Runoff Across Nine Mountainous Catchments. *Geophysical Research Letters*, *49*(13), e2022GL099324. https://doi.org/10.1029/2022GL099324

Stewart, I. T., Cayan, D. R., & Dettinger, M. D. (2005). Changes toward Earlier Streamflow Timing across Western North America. *Journal of Climate*, *18*(8), 1136–1155. https://doi.org/10.1175/JCLI3321.1

Sumargo, E., & Cayan, D. R. (2018). The Influence of Cloudiness on Hydrologic Fluctuations in the Mountains of the Western United States. *Water Resources Research*, *54*(10), 8478–8499. https://doi.org/10.1029/2018WR022687

Tennant, C. J., Crosby, B. T., & Godsey, S. E. (2015). Elevation-dependent responses of streamflow to climate warming. *Hydrological Processes*, *29*(6), 991–1001. https://doi.org/10.1002/hyp.10203

Thornthwaite, C. W., & Holzman, B. (1939). The Determination of Evaporation from Land and Water Surfaces. *Monthly Weather Review*, *67*(1), 4–11. https://doi.org/10.1175/1520-0493(1939)67<4:TDOEFL>2.0.CO;2

Udall, B., & Overpeck, J. (2017). The twenty-first century Colorado River hot drought and implications for the future. *Water Resources Research*, *53*(3), 2404–2418. https://doi.org/10.1002/2016WR019638

U.S. Geological Survey. (2016). *National Water Information System data available on the World Wide Web (USGS Water Data for the Nation),* [dataset].

Van Kirk, R. W., & Naman, S. W. (2008). Relative Effects of Climate and Water Use on Base-Flow Trends in the Lower Klamath Basin1. *JAWRA Journal of the American Water Resources Association*, *44*(4), 1035–1052. https://doi.org/10.1111/j.1752-1688.2008.00212.x

Vano, J. A. (2020). Implications of losing snowpack. *Nature Climate Change*, *10*(5), Article 5. https://doi.org/10.1038/s41558-020-0769-1

Vano, J. A., Das, T., & Lettenmaier, D. P. (2012). Hydrologic Sensitivities of Colorado River Runoff to Changes in Precipitation and Temperature. *Journal of Hydrometeorology*, *13*(3), 932–949. https://doi.org/10.1175/JHM-D-11-069.1

Vano, J. A., & Lettenmaier, D. P. (2014). A sensitivity-based approach to evaluating future changes in Colorado River discharge. *Climatic Change*, *122*(4), 621–634. https://doi.org/10.1007/s10584-013-1023-x

Vano, J. A., Udall, B., Cayan, D. R., Overpeck, J. T., Brekke, L. D., Das, T., Hartmann, H. C., Hidalgo, H. G., Hoerling, M., McCabe, G. J., Morino, K., Webb, R. S., Werner, K., & Lettenmaier, D. P. (2014). Understanding Uncertainties in Future Colorado River Streamflow. *Bulletin of the American Meteorological Society*, *95*(1), 59–78. https://doi.org/10.1175/BAMS-D-12-00228.1

Williams, A. P., Cook, B. I., & Smerdon, J. E. (2022). Rapid intensification of the emerging southwestern North American megadrought in 2020–2021. *Nature Climate Change*, *12*(3), Article 3. https://doi.org/10.1038/s41558-022-01290-z

Woodhouse, C. A., & Pederson, G. T. (2018). Investigating Runoff Efficiency in Upper Colorado River Streamflow Over Past Centuries. *Water Resources Research*, *54*(1), 286–300. https://doi.org/10.1002/2017WR021663

Woodhouse, C. A., Pederson, G. T., Morino, K., McAfee, S. A., & McCabe, G. J. (2016). Increasing influence of air temperature on upper Colorado River streamflow. *Geophysical Research Letters*, *43*(5), 2174–2181. https://doi.org/10.1002/2015GL067613

Xiao, M., Udall, B., & Lettenmaier, D. P. (2018). On the Causes of Declining Colorado River Streamflows. *Water Resources Research*, *54*(9), 6739–6756. https://doi.org/10.1029/2018WR023153

Yates, D., & Strzepek, K. (1994, July 1). *Potential Evapotranspiration Methods and their Impact on the Assessment of River Basin Runoff Under Climate Change*. https://www.semanticscholar.org/paper/Potential-Evapotranspiration-Methods-and-their-on-Yates-Strzepek/e6b3aceb2ddcd2b94afa301a3655efe8f4ad156b

Yin, J. H. (2005). A consistent poleward shift of the storm tracks in simulations of 21st century climate. *Geophysical Research Letters*, *32*(18). https://doi.org/10.1029/2005GL023684

Zhao, S., Fu, R., Anderson, M. L., Chakraborty, S., Jiang, J. H., Su, H., & Gu, Y. (2023). Extended seasonal prediction of spring precipitation over the Upper Colorado River Basin. *Climate Dynamics*, *60*(5), 1815–1829. https://doi.org/10.1007/s00382-022-06422-x

Zhao, S., Fu, R., Zhuang, Y., & Wang, G. (2021). Long-Lead Seasonal Prediction of Streamflow over the Upper Colorado River Basin: The Role of the Pacific Sea Surface Temperature and Beyond. *Journal of Climate*, *34*(16), 6855–6873. https://doi.org/10.1175/JCLI-D-20-0824.1

Zhao, W., & Khalil, M. a. K. (1993). The Relationship between Precipitation and Temperature over the Contiguous United States. *Journal of Climate*, *6*(6), 1232–1236. https://doi.org/10.1175/1520-0442(1993)006<1232:TRBPAT>2.0.CO;2